Universidade de Aveiro Secção Autónoma de Ciências da Saúde
2015

Sérgio Paulo Soares Reguengo

Complexos fosfodependentes na Thr668 da Proteína Precursora Amiloide

Amyloid Precursor Protein Thr668 phosphodependent complexes

Universidade de Aveiro Secção Autónoma de Ciências da Saúde
2015

Sérgio Paulo Soares Reguengo

Complexos fosfodependentes na Thr668 da Proteína Precursora Amiloide

Amyloid Precursor Protein Thr668 phosphodependent complexes

Dissertação apresentada à Universidade de Aveiro para cumprimento dos requisitos necessários à obtenção do grau de Mestre em Biomedicina Molecular, realizada sob a orientação científica da Professora Doutora Odete Cruz e Silva, Professora Auxiliar com Agregação da Secção Autónoma de Ciências da Saúde da Universidade de Aveiro.

Este trabalho contou com o apoio do grupo de Neurociências e Sinalização, Departamento de Ciências Médicas e Instituto de Biomedicina - iBiMED, Universidade de Aveiro e foi financiado pelos fundos JPND/0006/2011 BiomarKAPDua e PEST-OE/SAU/UI0482/2011.

Dedico este trabalho aos meus pais e irmão pelo incansável apoio ao longo desta jornada.

o júri

presidente

Doutora Sandra Maria Tavares da Costa Rebelo
Professora Auxiliar Convidada, Universidade de Aveiro

Professora Doutora Etelvina Maria de Almeida Paula Figueira
Professora Auxiliar, Universidade de Aveiro

Professora Doutora Odete Abreu Beirão da Cruz e Silva
Professora Auxiliar com Agregação, Universidade de Aveiro

agradecimentos

Um agradecimento muito especial à Professora Doutora Odete da Cruz e Silva, pela oportunidade de trabalhar no laboratório de neurociências e sinalização e pela orientação, conselhos, dedicação e paciência durante a realização desta dissertação.

À Professora Sandra Rebelo, pela ajuda e apoio que disponibilizou durante a fase final da realização desta dissertação.

Ao antigo CBC e atual iBiMED e à Universidade de Aveiro, pelos equipamentos e reagentes disponibilizados.

Um especial agradecimento ao Professor Doutor Jens Wiltfang, por me ter dado uma oportunidade no seu laboratório de Psiquiatria e Psicoterapia em Göttingen (mesmo em tempo de mudanças), pelos conselhos, apoio e interesse sempre disponibilizado. Ao Doutor Hermann, Doutor Hans, Doutor Oliver, Inga e Christin, por toda a ajuda, companheirismo e conselhos que me deram durante a minha estadia. Um agradecimento especial ao Professor Doutor Tiago Outeiro, pela disponibilização do microscópio de fluorescência em alturas de necessidade.

A todos os meus colegas de laboratório de neurociências e sinalização, que sempre estiveram disponíveis para conviver e ajudar, fosse qual fosse a situação. Um muito obrigado à Joana Oliveira, Joana Rocha, Filipa Martins e Roberto Dias, por me ajudarem em muitas das fases de realização desta dissertação.

Aos meus companheiros de licenciatura e mestrado. Ao Zé, Helder, Márcio, David e Vitor, pela amizade e por todas as histórias partilhadas ao longo deste tempo. À Soraia, pela amizade, paciência e pelos uteis conselhos ao longo deste ano. À Joana Serrano e à Catarina, pela sua amizade e boa disposição. À Joana Rodrigues, pela amizade e partilha de experiências.

Aos amigos que fiz na Alemanha, os quais tornaram a minha estadia o mais confortável e agradável possível. Um muito obrigado à Isabel, companheira inseparável, à Mariana, Rayne, Cátia e Gabriela; ao Sócrates e à Adriana.

Ao Sérgio, Daniel e Tânia, por fazerem do fim-de-semana um tempo de descanso necessário e recheado de bons momentos.

Aos meus pedaços (Hugo, Tiago, João Fernandes, João Medeiros), ao Pedro, Diana, Mário, Ana Rita, Igor, Lemos, Mega e restante comunidade de Ciências Biomédicas, pelas amizades e pelo constante interesse demonstrado sobre o meu trabalho.

Aos meus pais, irmão e família, pelo apoio incondicional ao longo dos anos. Sem eles, isto teria sido muito mais complicado.

palavras-chave

Doença de Alzheimer, células SH-SY5Y, Proteina Precursora Amiloide, Treonina668, Aβ, co-localização, fosforilação, complexos proteicos

resumo

A Doença de Alzheimer tem como uma das suas características principais, os depósitos do péptido tóxico Aβ, conhecidos como placas senis (PS). O péptido tóxico é produzido por complexas vias intracelulares e clivagens da Proteína Precursora Amiloide (PPA). Vários aspetos são importantes para o processamento da PPA. Entre eles, as proteínas que se ligam à PPA e formam diferentes complexes que são funcionalmente relevantes. Estudos recentes demonstraram que o estado de fosforilação da própria PPA é determinante para a formação desses complexos. Portanto, o estado de fosforilação da PPA determina o seu próprio destino, o rácio de produção de Aβ e a formação de placas senis. É também digno de nota que pacientes com mutação Swedish produzem cerca de 10 vezes mais Aβ.

O objetivo desta tese é considerar os fatores acima mencionados que modulam a produção de Aβ numa perspetiva única. Ou seja, considerar como a fosforilação da PPA afeta a produção de Aβ, tendo em conta o próprio estado fosforilado da proteína e os complexos proteicos que dai são formados. De modo a responder a essas questões, várias ferramentas biológicas tem que ser disponibilizadas. Consequentemente, esta tese propõem-se a preparar mutações Swedish na PPA (para produzir 10 vezes mais Aβ), a partir de cDNA da PPA que expressa mutações que imitam a fosforilação da Thr668. Este objetivo foi conseguido e foi possível demonstrar que as referidas mutações produziram níveis consideravelmente altos do péptido tóxico. Estudos preliminares de imunocitoquímica permitiram avaliar a distribuição celular dos mutantes produzidos, bem como da PP1γ em células SH-SY5Y, mas mais estudos são necessários para avaliar a co-localização do complexo proteico trimérico entre os mutantes da PPA, PP1γ e Fe65.

Assim sendo, estudos adicionais poderão contribuir para um melhor conhecimento da maneira como a produção de Aβ é influenciada por complexos proteicos regulados pela fosforilação da PPA.

keywords

Alzheimer's Disease, SH-SY5Y cells, Amyloid Precursor Protein, Threonine668, Aβ, co-localization, phosphorylation, protein complexes

abstract

Alzheimer's disease has as one of its characteristic hallmarks, deposits of a toxic peptide Aβ, known as senile plaques (SP). The toxic peptide is produced via complex intracellular pathways and cleavage of the Alzheimer's Amyloid Precursor Protein (APP). Several aspects are key to APP processing. Among them, the proteins that bind to APP and form different complexes, which are functionally relevant. Recent studies have shown that the phosphorylation state of APP itself is determinant with respect to the protein complexes formed. Thus the protein's phosphorylation state ultimately determines its own fate, the rate of Aβ production and the formation of SPs. It is also noteworthy the patients with Swedish mutation produced 10 times more Aβ.

The aim of this thesis is to consider the above mentioned factors, which modulate Aβ production in a unified perspective. That is, to consider how protein phosphorylation affects Aβ production, bearing in mind the phosphorylated state of the protein itself and the complexes that are formed. In order to address these questions, several biological tools have to be available. Hence this thesis set out to prepare the APP Swedish mutations (to produce 10 times more Aβ) on a cDNA which also expressed phosphorylation site mutations on APP Thr668. This was achieved and it was possible to demonstrate that the resulting mutations did in fact produce considerably higher levels of the toxic peptide. Preliminary immunocytochemistry studies allowed for assessment of cellular distribution of the mutants and PP1γ in SH-SY5Y cells, and more studies are needed to assess the co-localization of the trimeric protein complex between the APP mutants. PP1γ and Fe65.

Therefore additional studies could contribute to a better understanding of the way that Aβ production is influenced by protein complexes regulated by APP phosphorylation.

Index

List of figures

List of tables

List of abbreviations

A	Aβ	Amyloid beta-peptide
	AD	Alzheimer's disease
	ADAM	A disintegrin and metalloproteinase
	AICD	APP Intracellular Domain
	APBA1	Amyloid Precursor Protein-binding family A member 1
	APBB1	Amyloid Precursor Protein-binding family B member 1
	APBB2	Amyloid Precursor Protein-binding family B member 2
	APH-1	Anterior Pharynx-defective-1
	APLP1	APP-like protein 1
	APLP2	APP-like protein 2
	APOA1	Apolipoprotein A-I
	APOE	Apolipoprotein E
	APP	Amyloid Precursor Protein
B	BACE1	B-site APP cleaving enzyme
	BBB	Blood Brain Barrier
	BCA	Bicinchoninic Acid
	BLMH	Bleomycin hydrolase
	BSA	Bovine Serum Albumin
C	CALR	Calreticulin
	COL18A1	Collagen alpha-1 (XVIII) chain
	CNS	Central Nervous System
	CSF	Cerebrospinal Fluid
	CT	Computerized Tomography
	CTF	Carboxyl Terminal Fragment
	CTSD	Cathepsin D
E	ECL	Enhanced Chemiluminescence
	ER	Endoplasmic Reticulum

F	FAD	Familial Alzheimer's disease
	FLOT1	Flotillin-1
	FOS	Proto-oncogene c-Fos
G	GFP	Green Fluorescence Protein
	GPI	Glycosylphosphatidylinositol
	GPR3	G-protein coupled receptor3
H	HDL	High Density Lipoprotein
	HOMER3	Homer protein homolog 3
	HRP	Horseradish Peroxidase
	HSD17B10	3-hydroxyacyl-CoA dehydrogenase type-2
I	IDE	Insulin-Degrading enzyme
	ISF	Interstitial Fluid
	ITM2A	Integral membrane protein 2A
J	JUN	Transcription factor AP-1
K	KPI	Kunitz Protease Inhibitor
L	LB	Loading Buffer
	LDLR	Low-density lipoprotein receptor
	LRP	LDLR-related protein
	LTP	Long Term Potentiation
M	MAP3K5	Mitogen-activated protein kinase kinase kinase 5
	MAPT	Microtubule-associated protein tau
	MED12	Mediator of RNA polymerase II transcription subunit 12
	MRI	Magnetic Resonance Imaging
	MT-ND3	NADH-ubiquinone oxidoreductase chain 3

N	NEFL	Neurofilament light polypeptide
	NF1	Neurofibromin
	NFT	Neurofibrillary Tangles
	NGFR	Tumor necrosis factor receptor superfamily member 16
	NTF	Amino Terminal Fragment
O	OD	Optical Density
	ON	Overnight
P	PA	Phosphatidic acid
	PBS	Phosphate-buffered saline
	PCBD1	Pterin-4-alpha-carbinolamine dehydratase
	PCOLCE	Procollagen C-endopeptidase enhancer 1
	PDIA3	Protein disulfide-isomerase A3
	PEN-2	Presinilin enhancer-2
	PET	Positron Emission Tomography
	PFA	Paraformaldehyde
	PHF	Paired Helical Filaments
	PIN1	Peptidyl-prolyl cis-trans isomerase NIMA-interacting 1
	PKC	Protein Kinase C
	PP1	Ser/Thr Protein Phosphatase type 1
	PRNP	Major prion protein
	PS1	Presinilin 1
	PS2	Presinilin 2
	PSEN1	Presinilin 1 gene
	PSEN2	Presinilin 2 gene
	PVDF	Polyvinylidene Fluoride
R	RT	Room Temperature

S	SDS	Sodium Dodecyl Sulfate
	SHC1	SHC-transforming protein 1
	SHC3	SHC-transforming protein 3
	SLC40A1	Solute carrier family 40 member 1
	SPON1	Spondin-1
T	TGFB1	Transforming growth factor beta-1
	TGFB2	Transforming growth factor beta-2
	TGN	trans-Golgi-network
	TNFRSF21	Tumor necrosis factor receptor superfamily member 21
	TP53BP2	Apoptosis-stimulating of p53 protein 2
W	WB	Western Blot

1. Introduction

1.1. Alzheimer's disease (AD)

As the life expectancy of people around the world increases, it is projected that the number of elderly individuals developing dementia will also increase to 106 million worldwide by the year of 2050 (1,2). Dementia is characterized by a progressive decline in intellectual functions, such as memory, retention of information, attention and problem solving. This decline is only significant when it surpasses the normal changes related with the increase of age in normal individuals (3,4). Between all possible causes to develop dementia there are numerous neurologic diseases, such as frontotemporal dementia, dementia with Lewy bodies, vascular dementia, Alzheimer's disease, among others (2–5).

Alzheimer's disease (AD) is the most common cause of dementia in elderly people, constituting about 70% of all cases of dementia (5,6). In 2011, 25 million people were affected by AD worldwide (5). The first known case of AD occurred in 1907, when Alois Alzheimer studied a patient with symptoms like hallucinations and memory loss; the post-mortem examination revealed an evidently atrophic brain, with the presence of fibrils and deposits of a pathological material (5).

Since then, AD is clinically characterized by a progressive loss of memory, unusual behavior, dysfunction of personality and by a variability of other clinical findings associated with the affected brain regions, such as malfunctions in speech, vision and judgment, as well as mood changes (3,5,7). At a cerebral level, the brain of AD patients suffers a characteristic atrophy and mass loss, leading to an overall shrinkage, affecting specific areas like the cerebral cortex and hippocampus (4,8).

It is a progressive neurodegenerative disease, which starts as short-term memory loss episodes and with a slight decrease in the ability of performing simple and routine tasks , ultimately leading to a complete inability to live, culminating with death of the patients, due to other conditions, typically pneumonia, between 3 to 9 years after diagnosis (5,9). There is still no cure available at the moment (10).

1.1.1. Histopathological Hallmarks

On a cellular and molecular level, aside from loss of synapses, dendrites and neurons, there are two main histopathological hallmarks that define AD: intracellular neurofibrillary tangles (NFTs) and extracellular senile plaques (SP) (Figure 1) (5,8). These neuropathological findings present in the cortex and hippocampus of AD patients at higher levels than in the same age matched controls (7,11).

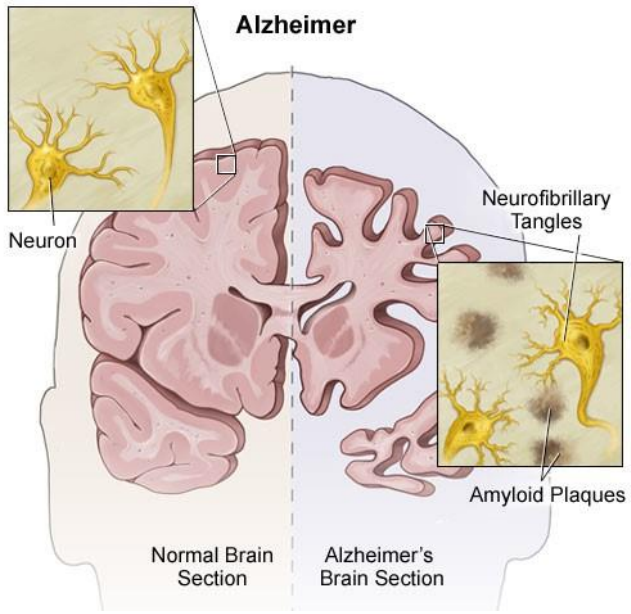

Figure 1 – Schematic representation of an AD brain and a normal brain.
The AD brain is represented on the right side and the normal brain on the left side. The neuronal structure is indicated as well as the site of NTF and SP deposits. A clear shrinkage is seen on AD brain section (taken from https://stanfordhealthcare.org/medical-conditions/brain-and-nerves/alzheimers-disease.html).

NFTs consists of intracellular aggregates of hyperphosphorylated microtubule-associated protein tau (7,12). Tau protein is regulated by its phosphorylated state. In normal conditions, this protein is not hyperphosphorylated and stabilizes neurons microtubules, especially in axons. When hyperphosphorylated, tau protein destabilizes microtubules by detaching from them and then accumulates to form insoluble tau aggregates into paired helical filaments (PHF). This leads to formation of NFTs in neurons of AD brains (7,12).

SP, on the other hand, are extracellular proteinaceous accumulations of a product of APP processing, amyloid beta (Aβ) peptides (12,13). This 4kDa peptide in its β-sheet

conformation is the main component of these large, dark and circular plaques (12). Aβ is found in healthy individuals as a normal physiological metabolite in an natively unfolded form (14–16). Not so much is known about its physiological function, only that it induces Long term potentiation (LTP) in hippocampus, and that the inhibition of its production leads to cell death. But as people age, changes occur in Aβ formation and metabolism, leading to the aggregation and deposition of Aβ in the form of plaques (SP) (15,17). This happens several decades before any clinical symptoms appear, and the observation of both SP and NTFs can only be confirmed *post mortem* (14,18). However, recent advances in diagnostic imaging are permitting earlier detection in the brains of AD patients, this is discussed below.

1.1.2. Epidemiology and Genetics

Over 25 million people in the world are affected by AD. Of all the cases, only 1 to 5% are due to mutations in specific genes (19). Normally, mutations in the amyloid precursor protein (APP), presinilin 1 (PSEN1) and presinilin 2 (PSEN2) genes, are all autosomal dominant, leading to premature onset of familial AD (FAD), that develop symptoms of AD before the age of 65 (19–21). The remaining AD cases represent sporadic forms of AD, in which the causes are not associated directly with any known mutation, are way more complex and implicate dysregulation of repair mechanisms, of cell metabolism and immune and inflammatory processes (13,21). However, the pathology of FAD and sporadic form of AD is very similar, comprising the same histopathological findings (22,23).

There are a lot of risk factors associated with AD. The main risk factor of AD, and the most often ignored, is the increase of age. As AD can occur around the age of 50, it suggests that the disease develops by some unknown age-related process. The risk is higher for individuals with age of 65 or older, and even higher above 85 years, when the risk increases almost 50 percent (24).

Other risk factors are known, including gender (females have a greater risk of developing AD), family history of dementia (patients with family members with AD are more likely to develop the disease), vascular changes, low level of education and genetic

and environmental factors (5,13,24,25). It is still unclear if smoking has some association with the development of AD (25).

In contrast, regular physical exercise and a cognitively stimulating environment are known to be neuroprotective, leading to enhanced brain activity and likewise neuronal survival and resistance (25,26).

1.1.2.1. Genetic risk factors

Aside from the previously referred mutations that will develop FAD, there are other genetic factors that will increase the risk of developing AD. The major genetic risk factor is apolipoprotein E (APOE) ε4 allele (27).

ApoE proteins (35-kDa, 299 amino acid) are members of the plasma lipid-binding protein family, present in higher concentrations in the liver and brain. These proteins are presented in High Density Lipoprotein (HDL)-like lipoproteins and are involved in transport and delivery of cholesterol and triglycerides between cells, regulating lipid homeostasis (18,28–30). It is produced mostly by astrocytes and is also implicated in removal of Aβ fragments by action of enzymes like neprilysin or by receptor-mediated uptake (18,31–33).

The APOE gene sequence is prone to variation, resulting in 3 types of alleles (ε2, ε3 and ε4). The alleles differ from one another in their amino acid composition at positions 112 and 158 (3,6,28). These simple amino acid differences change the structure of ApoE in a way that its ability to bind to lipids, receptors and Aβ is different between the existing isoforms (6,28,29). The ε4 allele of ApoE is known to be a major risk factor to develop AD, while the ε2 and ε3 allele are protective and the most common forms, respectively (28,34,35). Patients with two ε4 alleles (Homozygosity) have between 50% to 90% chance of developing AD until the age of 85, while the presence of only one ε4 allele (Heterozygosity) increases the chance to 45% (18,28).

ApoE is involved in Aβ metabolism and is a constituent of AD's SP, but its role in the development of the disease is still unknown (18,28). ApoE4's role in AD seems to be a combination of a gain in toxic function and loss of neuroprotective functions (28,29). The presence of ApoE4 highly influences and accelerates the formation of Aβ and its deposition into SP, this contrasts with the presence of ApoE3 (18,28). It appears that

ApoE4 is responsible for the initiation of SP formation in the brain (28). It is speculated that ApoE is a chaperone for Aβ fragments, regulating its conversion from an α-helix to a β-sheet conformation (6,18,30). The clearance of Aβ is also affected by the presence of ApoE4, leading to less efficient removal of Aβ and promoting Aβ aggregation and formation of senile plaques. ApoE4 is not so efficient in the removal of Aβ peptides when compared to ApoE3, which is consistent with ApoE4 having a lower affinity for Aβ peptides than ApoE3. Besides, elimination of Aβ peptides by specialized enzymes is confirmed to be more efficient with ApoE3 than with ApoE4, and reduced expression of those enzymes is observed in the presence of ApoE4 (6,18,28). Despite its important but unknown role in AD, the knockout of the APOE gene does not reveal improved neurological function, in part due to other types of lipoproteins acting in substitution of ApoE (6,13).

ApoE4 is not only related to Aβ metabolism. It also seems to have a role in inflammatory processes, initiating cascades that will culminate in neurovascular dysfunctions. Among these dysfunctions, the breakdown of the BBB and posterior leakage of blood toxins into the brain seem to be implied in the development of AD (28).

ApoE4 is the best characterized genetic risk factor, but mutations on other genes with a role in Aβ production and clearance also increase the risk of developing AD. This is the case for mutations in the SORL1, PICALM, CLU, CR1 or BIN1 genes (Table 1) (24,27).

Table 1 – Genetic factors associated with Alzheimer's Disease

GENE	GENETIC FORM	ONSET
AMYLOID PRECURSOR PROTEIN (APP)	Autosomal Dominant	Early
PRESENILIN 1 (PSEN1)	Autosomal Dominant	Early
PRESINILIN 2 (PSEN2)	Autosomal Dominant	Early
APOLIPOPROTEIN E4 (APOE4)	Familial and Sporadic	Late
SORTILIN-RELATED RECEPTOR L (DLR CLASS) A REPEATS-CONTAINING (SORL1)	Familial and Sporadic	Late
CLUSTERIN (CLU)	Sporadic	Late
PHOSPHATIDYLINOSITOL BINDING CLATHRIN ASSEMBLY PROTEIN (PICALM)	Sporadic	Late
COMPLEMENT COMPONENT (3B/4B) RECEPTOR 1 (CR1)	Sporadic	Late
BRIDGING INTEGRATOR 1 (BIN1)	Sporadic	Late

1.1.3. Diagnosis

Nowadays, the average span of time from diagnosis of AD to death is 4 to 8 years, despite the long time that the disease can take to run its course (around 20 years) (36). This means that diagnosis of AD is still done too late in the course of the disease (Figure 2). Diagnosing AD is difficult and most of the time unspecific. AD is still diagnosed by ruling out other neurologic disorders with similar symptoms, and the only way to definitely diagnosis the disease is by carrying out histological observation of the brain during autopsy (5,36).

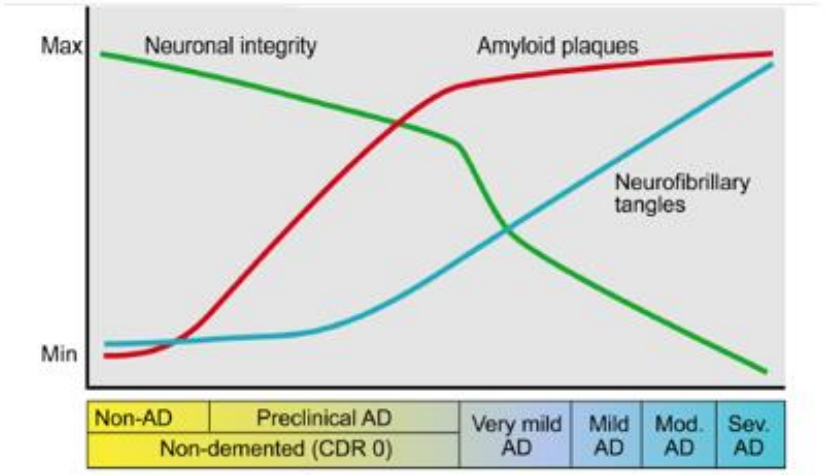

Figure 2 – Time course of AD's histopathological changes in relation to its clinical stages.
One of the first events that occur on normal people that will develop AD is aggregation of Aβ peptides in the form of SP. Over the years, SP continue to be formed, and tau accumulation begins to increase, leading to a moderate decrease of neuronal functions. As accumulation of Aβ and tau continues to increase, individuals start to lose its neuronal functions. AD's diagnosis occurs when Aβ accumulation is at its peak and neuronal integrity cannot be reversible (very mild AD) (taken from (30)).

However, new tools were developed that are now helping in the early diagnosis of this disease. Aside from an improvement in obtaining information by patient's and family's medical history, neurological examination and laboratory exams, neuroimaging techniques are improving drastically the diagnosis of AD. Techniques like Positron Emission Tomography (PET), Magnetic Resonance Imaging (MRI) or Computerized Tomography (CT) are now known as neuroimaging biomarkers in AD, providing structural and functional details of the patient's brain (5,37,38). Alternatively, AD biomarkers in Cerebrospinal Fluid [CSF] are presently being put into practice. The early detection of AD

patients can be carried out by testing the CSF for Aβ42 and phosphorylated and total tau protein (Table 2), but more biomarkers need to be identified and approved to allow for a better early detection, and to manage the progression of the disease, as well to generate new and efficient treatments (36,39). Currently, most AD biomarkers only indicate the risk of an individual to develop the disease, not the presence of the disease itself (27,36).

Table 2 – Fluid biomarkers of AD
Aβ1-42, total tau (t-Tau) and hyperphosphorylated tau (p-Tau) levels in plasma and CSF.

BIOMARKER	PLASMA	CSF
AB1-42	High	Low
T-TAU	Slight high	High
P-TAU	Slight high	High

Due to its prolonged development, increasing prevalence, difficult and unspecific diagnosis and high costs to the health systems and families, AD is now considered a major worldwide public health issue (14,18). Regrettably, to date there is no cure or way to prevent this disease, and the causes are yet to be fully understood (3,14). Current treatments focus in delaying of disease progression, management of symptoms and neuroprotective approaches in order to maintain a good mental function (40). In the future, AD's therapies will mostly rely on anti-amyloid therapies, by reducing Aβ production or increasing Aβ clearance.

1.2. Amyloid Precursor Protein (APP)

Human APP is a type I transmembrane protein, in the same family as APP-like protein 1 (APLP-1) and APP-like protein 2 (APLP-2). It has a large extracellular amino-terminal portion, and a short intracellular carboxyl-terminal portion (41–43). Human APP is encoded by the *APP* gene, located on chromosome 21. Due to alternative splicing of exons 7 and 8, APP exhibits three major isoforms that differ in the number of amino acids: APP695, APP751 and APP770 (Figure 3) (43–45). These APP isoforms are expressed in different types of tissues: APP695 is mostly expressed in neurons, while APP751 and

APP770 are expressed in all kinds of tissues (23,43). Whereas APP751 and APP770 have a Kunitz Protease Inhibitor (KPI) domain in their extracellular region, APP695 lacks that same domain (43). Among a lot of domains located in the N-terminal portion of APP, the most well-known and studied is the Aβ domain (41,46).

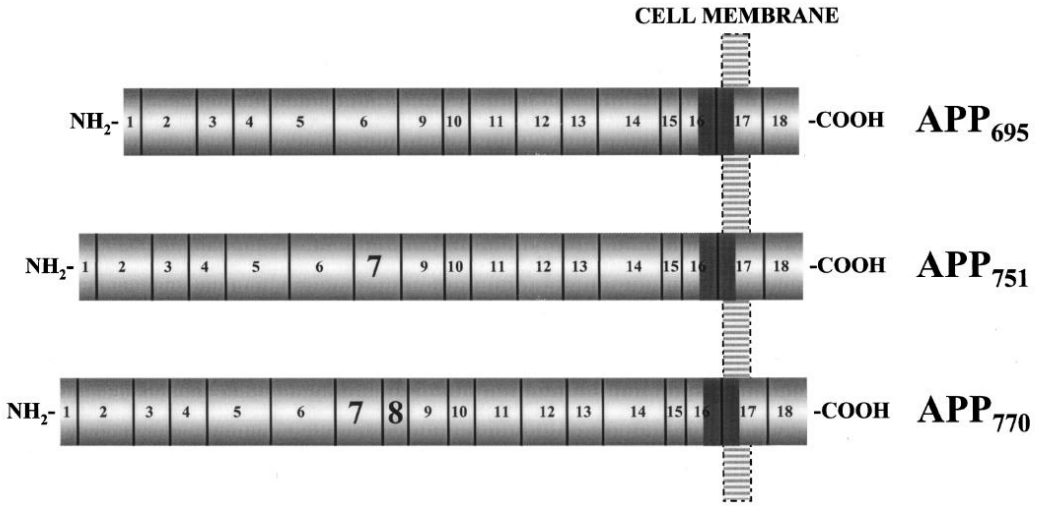

Figure 3 – Schematic representation of major APP isoforms in mammalian tissues.
Numbers and vertical lines show the corresponding exons approximately at scale. APP695, comprising 695 amino acids, is the most abundant APP isoform. APP695 do not express exons 7 and 8, unlike APP751 and APP770. APP751 differ from APP770 due to alternatively splicing of exons 7 and 8, as shown. Aβ region is represented as a solid black region between exons 16 and 17 (taken from (45)).

The Aβ domain has part of its peptides embedded within the membrane (26). When cleaved by specific secretases, the Aβ fragment is released in an unfolded state (14). This fragment can have different lengths (37 to 43 amino acids) depending on the site of cleavage by γ-secretases (Figure 4) (42). The most abundant Aβ fragment is Abeta40 (40 amino acids), but the most toxic Aβ fragment is Abeta42 (42 amino acids), probably due to its capacity to form oligomers and protofibrils faster than the other peptide species (9,14,42). The role of Aβ peptides in the development of AD has not been totally elucidated, and current theories point Aβ peptides oligomerization , contributing to rapid calcium leakage or to mitochondrial dysfunction, while several neuronal receptors have been discovered to bind Aβ peptides (14,33).

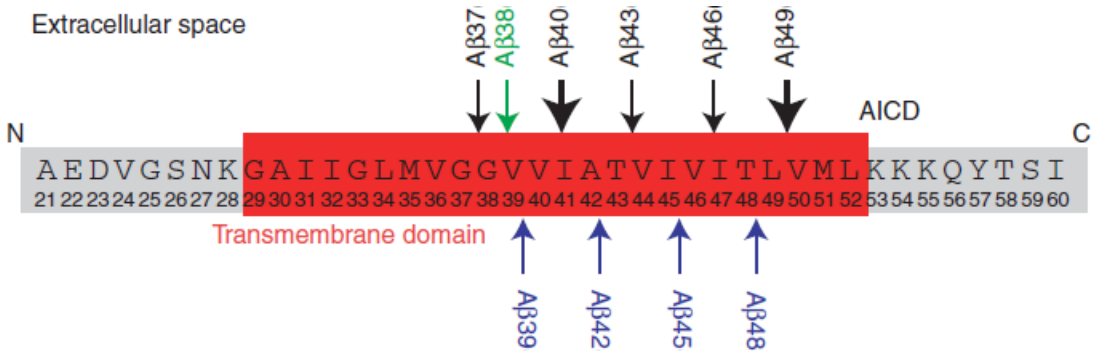

Figure 4 – γ -Secretase cleavage sites.
APP processing by gamma-secretase is not limited to only one site. The final cleavage by gamma-secretase is not precise and can take place at least between amino acids 37 and 43 of the A Beta domain, producing A Beta peptides with different lengths (adapted from (42)).

1.2.1. APP synthesis and transport

Full-length APP (110kDa) is synthesized in the Endoplasmic Reticulum (ER). Following its synthesis, it is transported to and through the Golgi apparatus until it reaches the trans-Golgi-network (TGN), where in neurons, it is found at its highest concentration (Figure 5) (42,43). From here, a small fraction (10%) of APP is directed to the surface of the plasma membrane, being transported in secretory vesicles derived from TGN by the anterograde transport system (11,42,43). Having reached the plasma membrane, APP can either be cleaved by cell-membrane secretases or be internalized within minutes of arrival via the endosomal systems (42,43). Endocytosis of APP is possible due to the "YENPTY" motif present near its C-Terminus. This motif is involved in clathrin-coated vesicle internalization (23). APP is transported to endosomes (Figure 5), where it can be recycled to the plasma membrane or be delivered to lysosomes to degradation (11,42).

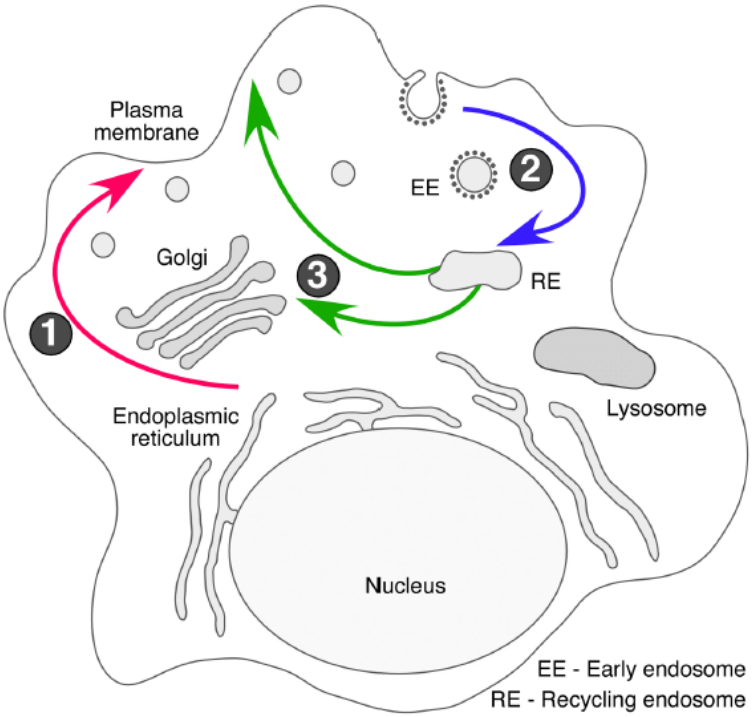

Figure 5 – Schematic illustration of intracellular trafficking of APP
1) Nascent APP matures through the constitutive secretory pathway until it reaches the plasma membrane; 2) On the plasma membrane, APP is rapidly internalized and 3) is trafficked through endocytic and recycling compartments back to the plasma membrane or to lysosomes, to be degraded (taken from (11)).

APP is concentrated in lipid rafts (LR) (Figure 6). LR are small membrane microdomains (~50nm) enriched with cholesterol, sphingolipids, proteins, and have a small amount of gangliosides (47–49). They are described as highly dynamic domains, with a nanoscale dimension, present abundantly in the plasma membrane (47,48). About 30 to 70% of the plasma membrane surface is constituted of LR, despise their small size (50,51). They function as membrane platforms that incorporate specific proteins of the membrane bilayer needed to initiate cellular functions (47,48). LR seem to be involved in apoptosis, cell polarization, adhesion and movement, regulation of endo and exocytosis, vesicular trafficking, membrane and protein sorting, cell migration and initiation of cell signalling pathways (47,48,51–53).

Several types of protein reside in the inner or outer leaflet of the LR (Figure 6). Proteins linked covalently to glycosylphosphatidylinositol (GPI) are a major component of the outer leaflet, while the inner leaflet of LR is filled with singly or multiply acylated

proteins (e.g. G-proteins. tyrosine kinases, protein phosphatases) (35,52,54). Numerous protein receptors are also found in LR, such as PDGF, EGF or cytokine receptors, as well as protein channels (44,54,55). Transmembrane proteins, like APP, are highly expressed in LR due to specific sequences in their extracellular, intracellular or transmembrane domain (50,56).

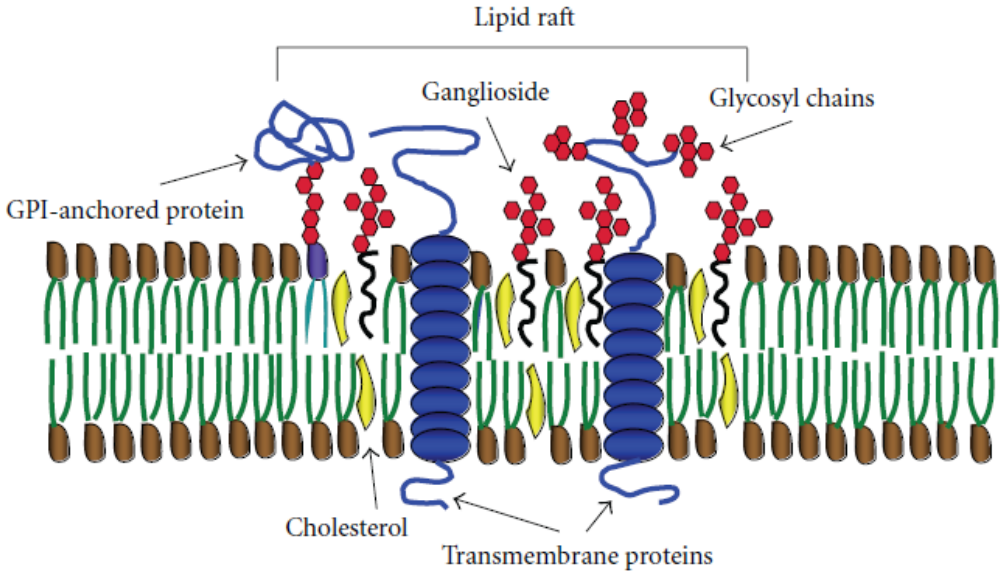

Figure 6 – Schematic representation of a membrane lipid raft.
Lipid rafts are small membrane microdomains enriched in gangliosides, cholesterol and sphingolipids (the last one is not represented on the figure). Several types of proteins are associated with lipid rafts, like GPI-anchored proteins and transmembrane proteins (taken from (48)).

1.2.2. APP proteolytic processing

APP is a highly expressed protein in neurons and is rapidly metabolized (23). Two distinct pathways can process APP: the amyloidogenic and the non-amyloidogenic pathway; both occur in cellular membranes, most specifically in lipid rafts. Lipid rafts, as said before, are membrane microdomains rich in cholesterol and sphingolipids. This special composition makes these domains prone to attract some types of proteins in preference to others, thus favoring some cellular processes. Regarding AD, lipid rafts are a subcellular site where most of the APP processing players coexist. To be more precise, APP, β-secretases and γ-secretases have all been found in lipid rafts (31).

The two, above mentioned, processing pathways share some common players, these compete with each other in certain subcellular compartments and contribute to the relatively short half-life of APP (42,57).

The amyloidogenic pathway leads to formation of Aβ fragments (Figure 7). APP is first cleaved by the action of a β-secretase. This secretase releases a large portion of the ectodomain of APP. The soluble fragment released is called sAPPβ (41,58). After β-cleavage, the remaining fragment of APP, a 99 amino-acid Carboxyl Terminal Fragment (CTF), called C99 (12 kDa), is still attached to the membrane (43,57–59). This C99 will be cleaved by a γ-secretase, releasing 2 more fragments: Aβ and the APP Intracellular Domain (AICD) (43,57,58).

The non-amyloidogenic pathway does not produce Aβ fragments (Figure 7). Instead of being cleaved by a β-secretase, APP is first cleaved by α-secretase (14,58). α-secretase cleaves within the Aβ region (between Lys16 and Lys17), preventing the formation of Aβ fragments. The soluble fragment released will also be different, in this case it is denominated sAPPα (14,44,58). sAPPα differs from sAPPβ because the first contains the Aβ 1-16 region at its C-Terminus, due to the α-secretase cleavage (43). The fragment that remains in the membrane is known as C83 (10 kDa), due to its 83 amino-acid constitution (57,58). C83 then suffers the same fate as C99: cleavage by a γ-secretase, releasing p3 (3 kDa) and AICD fragments (57,58). The p3 fragment seems not to be pathological (42).

Additionally, APP can be processed at its C-Terminus by the action of caspases like caspase-3, -6 and -8, resulting in a C31 peptide that seems to be an inducer of apoptosis.

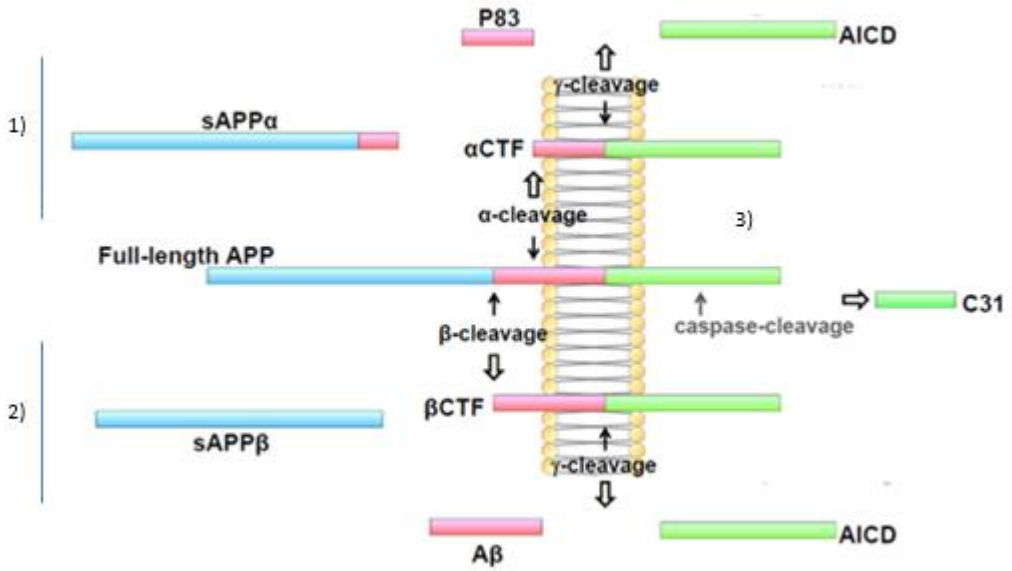

Figure 7 – Schematic diagram of APP proteolytic processing.
Three different APP processing pathways are represented. The first is the non-amyloidogenic pathway (1), in which alpha-secretase enables the secretion of sAPP alpha into the extracellular space, while the action of the gamma-secretase complex will release the p83 (or p3) and AICD fragments The amyloidogenic pathway (2) leads to the formation of A Beta instead of p3, due to the action of a Beta-secretase. APP can also be cleaved by the action of caspases (3), forming the C31 fragment. The different fragments are not drawn in proportion (adapted from (43)).

Although the formation of toxic Aβ fragments its said to be one of the leading causes of AD, α and β- secretase compete with each other for APP, and in 90% of the cases APP is cleaved by α-secretase (non-amyloidogenic pathway) (58,59).

Endocytosis also seems to have an important role in Aβ generation (44). Despite β-secretases and APP being confined to lipid rafts, this by itself is not enough to induce β-cleavage. Studies that inhibit cell endocytosis show no Aβ generation, but instead p3 production is enhanced, due to α-secretase occurring mostly at the cell surface (44,49). Endocytosis seems to be needed to further proceed in Aβ generation, supporting the theory that β-cleavage occurs in the last steps of the secretory pathway, mostly at the cell surface and during endocytosis, as described before (49).

1.2.2.1. β-secretase

In the brain, studies have shown that the major β-secretase is the β-site APP cleaving enzyme (BACE1) (41,43). BACE1 is characterized as a type I transmembrane

metalloproteinase, with its active site in the extracellular portion and found in high levels in neurons but at low levels in glia cells (23,42,58). BACE1 is generated from a large precursor (pro-BACE1) in the ER. This precursor is first modified by reactions of phosphorylation, palmitoylation, sulfation and glycosylation and finally is cleaved by a furin-like endoprotease in the Golgi, generating the mature BACE1 (70 kDa) (43,58,60). Both pro-BACE1 and BACE1 have protease activity and can mediate the first step in Aβ generation (58,60,61).

It is now known that BACE1 is the major β-secretase involved in APP processing and that it is essential to generate Aβ fragments (43,58,61). Due to its optimal activity in acidic environments (pH 4.5), BACE1 is mainly present in endosomes and early and late Golgi endosomes, snd co-localizes with APP-rich subcellular compartments. However, BACE1 can also be found on cell surface (23,43,58).

BACE was discovered to be present in lipid rafts; three of its cysteine residues are palmitoylated, which is a characteristic feature of lipid-raft associated proteins (59).

Consistent with APP being cleaved most of the time by α-secretases, and the fact that APP does not present the optimal cleavage site for BACE, others substrates of BACE1 have been discovered, such as APLP1, APLP2, sodium-channel β-subunit, neuregulin-1, low-density lipoprotein receptor (LDLR)-related protein (LRP), among others (15,58,60). This cogitates a normal function of BACE1 in the myelination process (42,60).

Another β-secretase that has been found, is BACE2. Although it has 60 to 70% of amino acid similarity with BACE1, this secretase is found in lower amounts in neurons when compared to BACE1 and it acts differently: it cleaves better near the α-secretase region than at the β-secretase region, eradicating Aβ production (43,58,60).

1.2.2.2. Gamma-secretase

γ-secretase is described as a multimeric protein complex with high molecular weight, that has in its composition four components: presinilin (PS1 or PS2), presinilin enhancer-2 (PEN-2), Nicastrin and anterior pharynx-defective-1 (APH-1) (23,43). All these four subunits are essential for enzymatic activity of the γ-secretase complex (Figure 8) (23,43).

Presinilins are multi-transmembrane proteins without a fixed number of transmembrane domains. There are two presinilins in mammals, PS1 and PS2. After being expressed, they suffer endoproteolytic cleavage. Then, a functional presinilin heterodimer is formed with the amino-terminal fragment (NTF) and the CTF produced by cleavage (42,43). Due to its two highly conserved aspartate residues, and the fact that the presinilin heterodimers are connected to γ-secretase inhibitors, presinilins are known to be the catalytic subunits of γ-secretase (43). Nicastrin, a type I transmembrane protein, is the recruiting protein of the γ-secretase complex that will bind to APP and other substrates, recruiting them to the multimeric complex (43). The main function of APH-1 is to interact with Nicastrin and stabilize it, while PEN-2 has a regulatory function in the γ-secretase complex, initiating the cleavage of PS1 or PS2 to form the PS heterodimer (23,42,43).

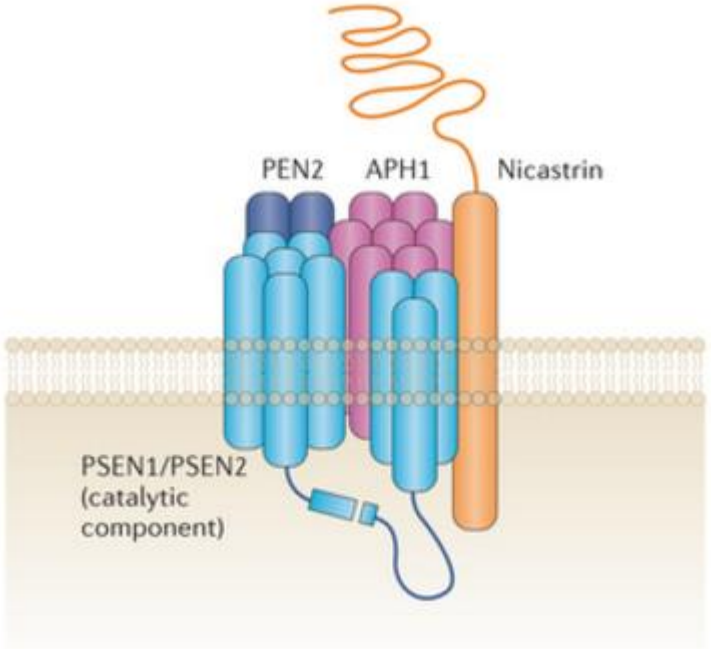

Figure 8 – Schematic diagram of the gamma-secretase complex.
The gamma-secretase is a multi-protein complex responsible for the intramembrane proteolysis of several proteins. It is constituted by a catalytic subunit (PSEN1/PSEN2), a recruiting subunit (Nicastrin), a scaffold subunit (APH1) and a subunit responsible to the endoproteolysis of PSEN1/PSEN2 (PEN2) (adapted from (85)).

Apart from these four components, other factors have been proposed to be part of the γ-secretase complex. However, these factors seem to play a support role instead of being essential for γ-secretase activity (43).

The γ-secretase multimeric complex has a specific subcellular localization: is mostly located in the plasma membrane, ER, endocytic compartments and Golgi apparatus (especially in TGN) (42,43). The γ-secretase complex is also found in lipid rafts, due to posttranslational palmitoylation (14,59). The process of palmitoylation seems to be crucial in the stabilization of Nicastrin and Aph-1 (44).

γ-secretase has some substrates beyond APP, such as Notch, cadherin or CD44 (43). Notch is mostly cleaved at the plasma membrane, while APP generally suffers its final cleavage at endocytic vesicles and at the TGN. This demonstrates that cleavage of γ-secretase substrates is reliant on the specific subcellular compartments that they share (42,43).

In the final step of APP processing, the protein site where γ-secretase will act is not precise, it appears that the Aβ cleavage site is in the sequence between amino acids 37 and 43, leading to the production of Aβ fragments of different sizes (42).

1.2.2.3. Alpha-secretase

α-secretase is a membrane-bound zinc metalloproteinase found essentially at the plasma membrane of cells (43,44). Its characterized as a type-I transmembrane protein, like APP, and is involved in the non-amyloidogenic pathway APP processing (43).

There is no consensus to define the principal α-secretase involved in APP processing. Some ADAM (a disintegrin and metalloproteinase) family members have α-secretase activity and have been proposed to be the main α-secretase in APP processing (43,44). These include ADAM9, ADAM 10 and ADAM17. Studies points to ADAM10 being the main α-secretase at the cell surface, but depletion of any of the ADAM proteins will decrease Aβ formation. Due to these findings, functional redundancy in α-cleavage leads to the theory that there is likely to be more than a single α-secretase involved in APP processing (43,44).

α-secretase is allegedly found in non-rafts portions of the cell membrane (18,33,44). Despite APP being associated with lipid rafts, α-secretase activity accounts for more than 90% of APP processing. This can be explained by the existence of two cellular pools of APP, one directed to lipid rafts and the other associated with the non-raft parts of the membrane (14,44,59).

Alongside APP, other substrates are cleaved by α-secretases. All kinds of type I transmembrane proteins are substrates for α-secretases, such as Tumor necrosis factor α, the pion protein, Notch receptors and ligands or cadherins (42,44).

1.2.3. Aβ clearance

As discussed above, Aβ peptides can be found in healthy patients, and it is presumed to have a physiological role (29). As such, it is normal that the brain has mechanisms to eliminate Aβ peptides, which have a half-life of approximately 8h in human brains (29).

Aβ peptides can be eliminated by various ways: proteolytic degradation by action of enzymes; clearance mediated by receptors in neuronal cells (neurons, glia cells); through the Blood Brain Barrier (BBB) or through the Interstitial fluid (ISF) drainage pathway (Figure 9) (6,29).

Aβ clearance is mediated by receptors in neuronal cells or even on endothelial cells that form the BBB. The receptors that seem to be involved are likely to be ApoE-lipoprotein receptors (LDLR family members) which are widely present in the cell types previously reported (6,29). Aβ peptides are then internalized together with the receptors in endosomes and delivered to lysosomes where they can be degraded (29). This method has proved to be reliable to eliminate the Aβ peptides, but is possible that it could lead to toxic intracellular accumulation of those peptides in multivesicular bodies, endosomes and lysosomes (29).

Another method of Aβ clearance is by proteolytic degradation via the action of Aβ-degrading enzymes (6,29). The enzymes are produced and expressed in both neurons and glia cells and in to some extent in the cerebral vasculature (29). Several enzymes have been associated with this process, and Neprilysin and Insulin-Degrading enzyme (IDE) are among the most studied ones (6,29).

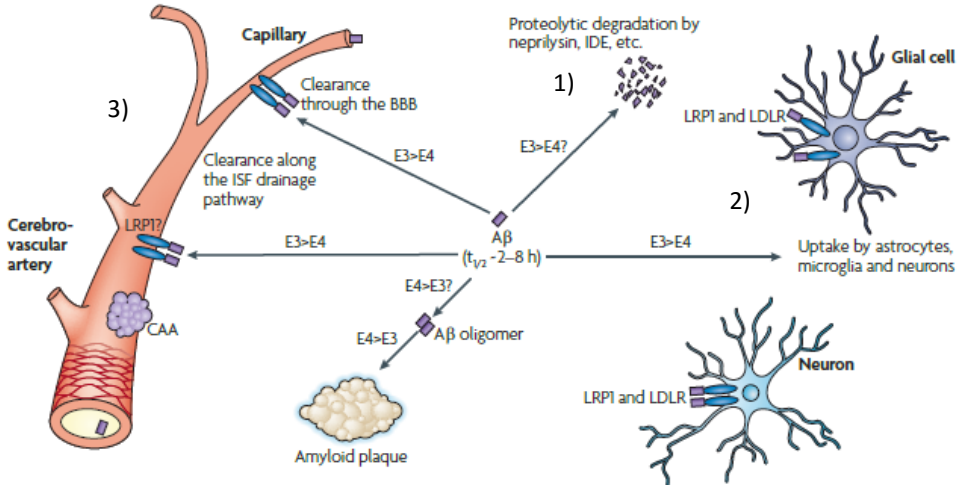

Figure 9 – Aβ clearance pathways in the brain.
A Beta peptides accumulation in the brain leads to A Beta oligomerization and formation of senile plaques (SP). A Beta has a short half-life in the brain of humans (~8h). The major Abeta clearance pathways are shown: proteolytic degradation by action of enzymes (1); clearance mediated by receptors in neuronal cells (2) and clearance through the Blood Brain Barrier (BBB) or the Interstitial fluid (ISF) drainage pathway (3) (adapted from (29)).

1.2.4. APP phosphorylation

Among all the regulatory mechanisms in cell biology, protein phosphorylation is the major one, it is involved in all kinds of cell functions (45,62). Typically, a protein kinase transfers a phosphate molecule from an ATP molecule to a protein. This will lead to alterations in the conformation of the protein, as well as its function. To revert to its original state, the phosphate molecule will be removed by the action of a protein phosphatase.

Despite being a highly regulated mechanism, protein phosphorylation is altered in many diseases, including AD (45,62). The brain has the highest concentration of protein kinases and phosphatases, and it can be explained by the fact that brain functions, like memory, are important and dependent on protein phosphorylation. So, an abnormal regulation of these processes will contribute to the development of AD.

Apart from tau protein which is found hyperphosphorylated in AD, phosphorylation of APP may also contribute to the progression of the disease (62). APP is considered to be a phosphoprotein, so is natural that it would be affected by phosphorylation reactions. APP levels and functions (binding, trafficking and processing)

seem to be under regulation of both protein kinases (Protein Kinase C [PKC]) and protein phosphatases (Ser/Thr protein phosphatases type 1 [PP1]). Within its intracellular domain, APP presents 8 possible phosphorylation sites (Figure 10). In patients with AD, seven of those APP possible phosphorylation sites (Figure) were demonstrated to be phosphorylated *in vivo* and *in vitro*: Tyr653, Ser655, Thr668, Ser675, Tyr682, Thr686 and Tyr687 (in APP695 numbering) (33,49).

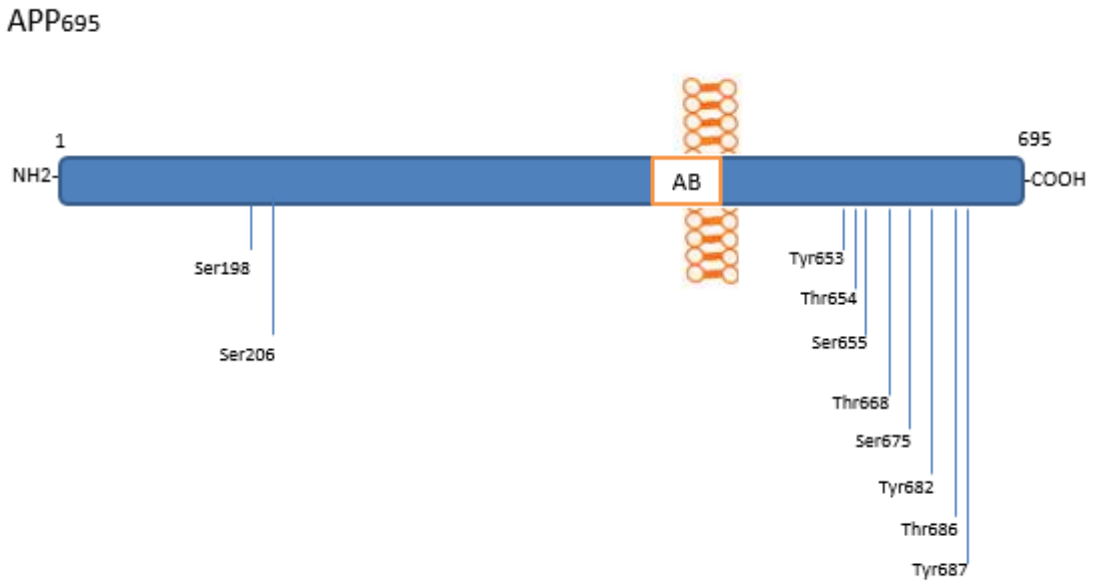

Figure 10 – Schematic representation of APP695 phosphorylation sites.
The eight putative phosphorylated sites in the APP intracellular domain and the two phosphorylated Ser residues in APP ectodomain are shown.

Regarding AD, patients exhibit an upregulation of APP βCTFs phosphorylated at Thr668. It is also found phosphorylated in rat brains and in several cell lines. Phosphorylation of APP at Thr668 is normally detected in the brain, and is associated with a role in APP metabolism, more specifically in making APP more favorable to be cleaved by BACE1 and forming Aβ fragments (49). Phosphorylation at Thr668 seems also necessary to form the interaction of AICD and Fe65, allowing AICD to be internalized into the nucleus and inducing neurotoxicity (64). Other putative roles of phosphorylation on this residue are related with regulation of neurite extension, of APP axonal trafficking and attenuation of APP cleavage by caspases. Both phosphorylated APP and CTFs at Thr668 are found at neurites within growth cones, while the dephosphorylated APP is found at its

highest in the neuronal cell body. Study of APP Thr668 phosphorylation can be made by replacing that residue with an Alanine or a Glutamate, to mimic both non-phosphorylated and phosphorylated state, respectively.

Another APP intracellular site, Tyr687, is also found phosphorylated in AD, and it seems to be involved in the subcellular localization of APP (62). Phosphorylation at Ser655 seems to regulate APP binding and APP secretory trafficking, while phosphorylation at Tyr682 promotes interactions between APP and Shc adapter proteins. Little information is found concerning the remaining APP intracellular phosphorylation sites (62).

Regarding the APP ectodomain, Ser198 and Ser206 are sites suffer phosphorylation, but they do not seem to be involved in AD related events (Figure 10) (65).

1.2.5. APP and APP fragments functions

The normal function of full-length APP is still unknown, but diverse studies suggest a role in synaptogenesis, neurite outgrowth, synaptic plasticity, regulation of neuronal survival, cell adhesion and in learning and memory processes (26,57). Another possible function of the full-length APP is that it can act as a cell surface receptor, but until now, no ligand nor related signaling pathway have been discovered (26,57).

Since its synthesis until it reaches the plasma membrane, APP goes through a lot of co- and post-translational modifications, such as phosphorylation, N- and O-glycosylation and tyrosine sulfation. However, it is on its way to and at the plasma membrane that APP is processed by endoproteolytic secretases into smaller and distinct fragments (11,21). The proposed functions of full-length APP seem to result from the sum of all related functions of the various APP peptidic fragments.

sAPPα seems to have a neuroprotective function, promoting neurite outgrowth, synaptogenesis, regulating calcium homeostasis and involvement in cell adhesion. However, sAPPβ does not have the neuroprotective effects of sAPPα, having instead functions related to neuronal cell death and stimulation of axonal pruning. The intracellular CTFs of APP do not have a specific function, but they have the ability to bind to several different proteins that will bind to effector proteins. AICD was shown to act as a

transcriptional factor. It is involved in a lot of functions that vary from cell migration and signaling to axonal transport and apoptosis due to the presence of a motif that will interact with a lot of adaptor proteins that will modulate all the cited functions (44,57). Upon its formation, AICD interacts and activates the nucleocytoplasmic adaptor Fe65 so it can bind with Tip60 and can enter the cell nucleus, exerting an effect at the level of the cell genome. It has been verified that AICD has transactivation activity regarding a vast group of genes like *APP*, *BACE1*, *LRP1*, *EGFR*, *neprilysin* and *p53* (43,44). The fact that APP and BACE1 expression are regulated by AICD provides information supporting a feedback mechanism whereby AICD regulates the processing of its precursor (44).

2. Aims of the dissertation

Alzheimer's disease (AD) is a complex neurodegenerative disorder characterized by a progressive loss of mental functions and reduction of the ability to perform simple daily activities. AD has two major histopathological hallmarks: extracellular senile plaques and intracellular NTFs. The Aβ peptide is the main component of the SP and is produced due to cleavage by β- and γ-secretases of the Amyloid Precursor Protein (APP). Aβ pathological levels seem to be altered when phosphorylation reactions occur in Threonine 668 of the APP. Several protein complexes seem to interact with APP, like the trimeric complex APP/PP1/Fe65. PP1 is the central phosphatase involved in dephosphorylation of APP and it was shown to bind with both APP as well as the adaptor protein Fe65 in a trimeric complex involved in APP processing. In the latter tricomplex, phosphorylation at APP Thr668 was shown to be an important regulatory event.

In this work the hypothesis that APP, via its interaction within different protein complexes, regulates Aβ production will be tested.

To support this hypothesis, the specific objectives will be:

- To characterize the APP Interactome;
- To construct APP Wild Type and Swedish Thr668 phosphomutants (Thr668A and Thr668E) thus mimicking both dephosphorylated and phosphorylated states;
- To optimize cell transfection with APP Thr668 phosphomutants;
- To study the effects of APP phosphorylation at Thr668 (mimicked by APP Wt and Swe Thr668 phosphomutants) regarding Aβ processing;
- To co-localize APP Thr668 phosphomutants with Fe65 and PP1γ.

3. Materials and Methods

3.1. Cell Culture

All methods involving cell culture and manipulation were performed using a class II air flow cabinet.

3.1.1. Culture, growth and maintenance of SH-SY5Y cell line

Due to being human derived cells, SH-SY5Y cell line was chosen as the model for all the procedures involving cells. SH-SY5Y human neuroblastoma cells are derived from the SK-N-SH cell line, established originally from a metastatic bone tumor biopsy (66).

SH-SY5Y cells were grown and maintained in 10% fetal bovine serum (FBS) Minimal Essential Medium (MEM)/F12 (1:1) with 0.5mM L-glutamine, 100 U/mL penicillin and 100 mg/mL streptomycin.

Cells were maintained in an incubator at 37ºC with 5% CO2/95% air and 95% humidity. When cells reached about 70-80% of confluence, they were passaged or used for experimental procedures. Standard laboratory procedures were used as previously described (62).

3.1.2. Transient transfection

SH-SY5Y cells were transfected with APP-GFP constructs using a cationic lipid reagent-mediated method (Lipofectamine 2000 reagent). The day before transfection, cell were plated on a 6-well plate with complete DMEM Medium.

On the next day, each cDNA and Lipofectamine 2000 were separately diluted in DMEM medium (serum free) for 5 min. The solution with cDNA was mixed in the Lipofectamine 2000 solution and left for 20 min at RT for DNA complexes to form. This mixture was then added to the medium of the respective plates of SH-SY5Y cells. The plates were then incubated at 37ºC and 5% CO2 for 8h. After that period, the DMEM medium (serum free) was discarded and new complete DMEM Medium was added.

3.2. Western Blot

Western Blot (WB) is a multistep technique for detection and characterization of proteins, widely used in experimental procedures. First, samples need to be collected and prepared, then separated on an electrophoresis gel and lastly transferred onto a

nitrocellulose membrane. Antibodies against the protein of interest will be added to the membrane, incubated, detected and finally analyzed (67).

3.2.1. Sample collection

Cell medium was collected into microtubes, and cells were first washed with PBS, and then harvested with 200 µL of 1% Sodium Dodecyl Sulfate (SDS). SDS is a strong and ionic detergent used to solubilize lipids and proteins in cell membranes. This leads to cell lysis by the formation of pores within the membrane.

Cell lysates were then collected and put on ice, boiled for 10 min and later sonicated 2 times for 3 seconds to homogenize the samples. All samples were stored at -20ºC before any experimental procedures.

3.2.2. Determination of protein concentration

Protein content quantification of cellular lysates was carried out using the BCA Protein Assay (Pierce). This assay combines the reduction of Cu^{2+} to Cu^{+} by cell proteins in an alkaline medium with a sensitive colorimetric detection of Cu^{+} cation with the use of a solution containing bicinchoninic acid (BCA). The purple-colored product is the result of the reaction between two molecules of BCA with one Cu^{+} ion. This complex is water soluble, exhibiting a strong absorbance at 562 nm that is linear with increasing protein concentration (67). The standards were prepared in a 96-well plate, as described in Table 3, and final volume of each well was equal to 25 uL. The procedures used are those well established in the laboratory (62).

Table 3 – Protein Standards used in BCA protein Assay method

Standard	BSA(µl)	10% SDS (µl)	Protein Mass (µg)
P0	-	25	0
P1	1	24	2
P2	2	23	4
P3	5	20	10
P4	10	15	20
P5	20	5	40

A microtube was prepared for every sample, with 5ul of each sample plus 20ul of the solution in which the sample was collected (1% SDS). After preparation of both standards and samples, the plate was incubated for 30 minutes at 37º C with 200 ul of working reagent (50 parts of reagent A to 1 part of reagent B). After incubation, the plate was cooled at RT for 5 minutes and then the absorbances were measured at 562 nm. A standard curve was made by plotting the Optical Density (O.D.) value for each BSA standard against its corresponding concentration, which was then used to determine the protein concentration of each sample. Both standards and samples were prepared in duplicate.

3.2.3. SDS-Polyacrylamide Gel Electrophoresis

SDS-Polyacrylamide gel electrophoresis (SDS-PAGE) is an analytical technique that allows the separation and characterization of proteins and peptides of a sample mixture in a polyacrylamide gel by application of an electrical current. SDS is as anionic detergent able to denature proteins by wrapping around their polypeptide backbone. This will confer a negative charge to the protein in proportion to its length, and so, sample proteins are separated according to their molecular weight and negative net charge (67).

Samples were subjected to a 5-20% gradient SDS-PAGE in a Hoefer electrophoresis system. This denaturing gel is used because it allows a separation of proteins based solely on their molecular weight. It consists of two similar gels, but with different polyacrylamide concentrations: the resolving gel (bottom) has a higher concentration of polyacrylamide than the stacking gel (top) (Table 4).

A loading buffer (LB) was added to the samples before loading onto the gel. This loading buffer consists of Glycerol, SDS. β-mercaptoethanol and bromophenol blue. Glycerol allows the sample to stay in the wells by increasing the sample density; SDS covers the inherent charge of the sample proteins; β-mercaptoethanol breaks the disulfide bonds that are present on the tertiary and quaternary protein structures; and the bromophenol blue is a dye needed to track the progression of the sample in the gel (67).

Table 4 – Stacking and resolving gel compositions for one SDS-PAGE system (1.5mm of thickness)

Reagents	Stacking Gel	Resolving Gel	
	3,5%	5%	20%
Water	13.83 mL	18.59 mL	7.34 mL
Acrylamide (29:1)	1.75 mL	3.75 mL	15 mL
LGB (4X)	-	7.5 mL	7.5 mL
UGB (5X)	4 mL	-	-
10% SDS	200 uL	-	-
10% APS	200 uL	150 uL	150 uL
TEMED	20 uL	15 uL	15 uL

Electrical current is applied to the gel for approximately 4 hours so it can enable the separation of the sample proteins. After gel separation, proteins are transferred electrophoretically onto a nitrocellulose membrane so that all proteins can be immobilized at their relative positions at the time point when the gel run was stopped.

3.2.4. Western Blotting Analysis

A wide number of antibodies were used to detect the protein of interest by immunological and chemiluminescent protein detection (Table 5).

Table 5 – Antibodies used to detect the proteins of interest

TARGET	*PRIMARY ANTIBODY*	*SECONDARY ANTIBODY*
AB N-TERMINAL	6E10 Dilution 1:1000	Horseradish Peroxidase conjugated α-mouse IgG Dilution 1:5000
APP C-TERMINAL	Anti-C-Terminal Dilution 1:1000	Horseradish Peroxidase conjugated α-rabbit IgG Dilution 1:5000
B-TUBULIN	Anti-β3-tubulin Dilution 1:1000	Horseradish Peroxidase conjugated α-mouse IgG Dilution 1:5000

Following transfer, the nitrocellulose membrane was hydrated with 1x TBS for 10 min, followed by blocking with 3% BSA in 1x TBS-T. This step is necessary for the blocking of possible non-specific binding-sites. Afterwards, the membrane was incubated with an unlabeled primary antibody (that will bind to the target protein) for 4 hours at RT, with agitation, followed by an ON incubation at 4º C. The membrane was then washed 3 times with 1x TBS-T (10 min each), incubated with the secondary antibody coupled with horseradish peroxidase (HRP) for 2 hours, and washed again 3 times with TBS-T for 10 minutes each.

For protein detection, the nitrocellulose membrane was then incubated with the enhanced chemiluminescence (ECL) reagent or with Limunata Crescendo in a dark room, for 1 and 5 minutes, respectively. This method relies on the oxidation of cyclic diacylhydrazide luminal that will produce light. The membrane was subsequently exposed to autoradiography films (Kodak) in X-ray film cassette, for different periods of time depending on the protein of interest. Finally, the films were developed and fixed with the appropriate solutions (Kodak) as specified by the manufacturer.

3.2.4.1. Membrane stripping

Proteins with similar molecular weights (KDa) can be visualized in the same blot with the method of membrane stripping in between the immunodetections.

A stripping solution PH 6.7 containing Tris Base and SDS was prepared and then mixed with β-Mercaptoethanol. After hydration of the nitrocellulose membranes with 1x TBS, the stripping solution previously prepared was added to the membrane, at 37ºC for 30 min with agitation. The stripping solution was then discarded and the membrane washed, first 3 times with 1x TBS-T and finally with distillated water. The membranes were left to dry at room temperature.

To confirm the stripping, membranes were first rehydrated with 1x TBS and then blocked with 5% BSA in 1x TBS-T solution for 1 hour. After, membranes were incubated with the secondary antibody and developed with ECL reagent, Luminata Crescendo.

3.2.4.2. Ponceau S staining

The nitrocellulose membrane was first incubated in a previously prepared Ponceau S solution during a short time (between 5 and 10 min) and then washed with deionized water to make the bands in the membrane more clearly visible. The membrane was scanned in a GS-800 calibrated imaging densitometer in order to evaluate equal gel loading. Lastly, the membrane was extensively washed with 1x TBS-T to remove the staining. The regions of interest of the membrane were used as a loading control.

3.2.5. Aβ-SDS-Polyacrylamide Gel Electrophoresis (Aβ-SDS-PAGE)

Separation of Aβ peptides is achieved by the use of a urea version of the Bicine/Tris SDS-PAGE. The use of urea will induce conformational changes in Aβ peptides, which differ in one or two amino acids. With this method, those Aβ peptides can be easily separated (68–70).

Cell medium samples were first immunoprecipitated to collect Aβ peptides. The immunoprecipitation was carried out using Dynabeads® Protein G (Invitrogen) magnetic beads. This will allow for a fast and efficient collection of our target protein and eliminate background since it will decrease the non-specific binding of proteins. The primary antibody (6E10) is added to the Dynabeads® Protein G. During a short incubation, the antibody will bind to the beads. Afterwards, the tube with the beads is placed on a Dynal magnet that will allow the capture of the beads with the antibody so that the supernatant can be easily removed. The beads were then stored in PBS 0,1% BSA, 0,02% NaN3 at 4º.

To cell medium samples (800ul), 200 ul of 5-fold concentrated IP detergent buffer (10% Nonidet P-40, 10% sodium deoxycholate, 10% SDS, 5M NaCl, 1M HEPES, one tablet of Roche Complete Protease Inhibitor Cocktail Mini per 2mL of final volume, pH adjusted to 7.4 with NaOH) were added. To this 25ul of activated and covalently coupled 6E10 beads were also added, and samples were incubated under rotation for 15h at 4º C. Beads were later washed 3x with PBS 0,1% BSA for 5 minutes each; once with 10mM Tris-HCL (pH 7.5). Bound Aβ peptides were then eluted by heating the sample to 95ºC for 5 min in 25ul of sample buffer (0,36M bis-Tris, 0,16M Bicine, 1% SDS, 15% sucrose and 0,0075% bromophenol blue). Beads were immobilized for 2 minutes and the supernatant with the Aβ peptides transferred to new tubes.

Immunoprecipitated samples were resolved on 12% Bicine/Tris gels containing 8M urea. Synthetic Aβ peptides (Aβ1-37, Aβ1-38, Aβ1-39, Aβ1-40 and Aβ1-42 by Annspec) were run in a different and parallel well with the purpose of identifying the different Aβ peptide species. A protein loading control (Precision Plus Protein® All Blue Standards) was also loaded. After gel separation, Aβ peptides were transferred under semidry conditions onto a methanol-activated Polyvinylidene Fluoride (PVDF) membrane so that all gel proteins can be immobilized at their relative positions at the time point when the gel run was stopped. Membranes were then washed with H2Odd and boiled for 3 minutes in PBS using a microwave oven. Blocking was performed for 1h at RT with Amersham ECL® Prime Blocking Reagent. After washing 3x with PBS-T, a primary antibody (6E10) was added to the membrane, incubated for 1h at RT, washed again 3x with PBS-T and incubated with a secondary antibody (MAB2) for 1h. The PVDF membrane was then incubated with Streptavidin-biotinylated horseradish peroxidase complex (GE Healthcare) for 1h at RT. Aβ peptides were visualized in the membrane using the LI-COR Odyssey Fc device after a short incubation with Amersham ECL® Start Western Blotting Detection for 5 minutes.

3.2.6. Bioinformatics tools

A wide set of bioinformatics tools were used: Protein-Protein interactions databases (UniProt, IntAct); web resources to draw protein networks (SPRING); and web resources to obtain information about protein properties (PANTHER). The FinchTV software was used to confirm the cDNA mutations.

3.3. Immunocytochemistry

Immunocytochemistry is a laboratory technique used to see proteins in cells. Proteins are visualized with the help of biomolecules capable of specifically binding the protein of interest; normally the biomolecule is an antibody linked with a reporter, which can be a fluorophore or an enzyme. The reporter will produce a signal (fluorescence or color) that is detectable with the use of an appropriate microscope that depends on the reporter type (71).

Immunocytochemistry was performed in order to visualize APP phosphomutants tagged with GFP as well as the proteins Fe65 and PP1γ. Cells were first plated and transfected into glass coverslips (15mm) for 24h. Cells on the coverslips were then fixed with a solution of 4% Paraformaldehyde (PFA) for 20 minutes at RT, and washed 3x with PBS to remove the fixing reagent. Following fixation, cells were first permeabilized with 0.2% PBS-Triton for 10 minutes, washed 3x PBS, and then blocked with a 3% BSA/PBS solution for 1h at RT.

Following those steps, cells were incubated with a primary antibody against the proteins of interest for 2h on humidified conditions (Table 6). The primary antibody is diluted in the blocking solution (3% BSA/PBS). Cells were washed 3x with PBS and then incubated with the fluorescently-labelled secondary antibodies diluted in 3% BSA/PBS for 1h in a dark environment (Table 6). Coverslips were washed again 3x PBS and 1x with distillated water. Following the washing steps, a drop of mounting medium (Vectashield without DAPI) was added to each slide.

Fluorescence microscopy was performed using an LSM510-Meta confocal microscope (Zeiss), and the argon laser lines of 405 nm, 488 nm and 561 nm DPSS laser were used. Pictures were acquired using the Zeiss LSM 510 4.0 software.

Table 6 – Primary and Secondary antibodies used in immunocytochemistry

Target	Primary Antibody	Secondary Antibody
Fe65	Anti-Fe65 (Mouse) Dilution: 1:250	AlexaFluor 594 (Mouse) Dilution: 1:300
PP1γ	Anti-PP1γ (Rabbit) Dilution: 1:500	AlexaFluor 405 (Rabbit) Dilution: 1:200

4. Results and Discussion

4.1. APP Interactome

Proteins interactomes are a crucial tool to understand the network of possible interactions between different proteins. Protein-protein interactions are the key to understanding cellular processes, thus interactomes are constructed to provide a useful insight into the mechanism of protein functions. Interactomes are dynamic: many interactions occur for a particular time in a protein life; others may be transient or can only happen under specific cellular contexts (72–74).

In order to construct the APP interactome, protein-protein interactions were obtained by using a primary database that contains protein-protein interactions. A large number of databases are available, but the UniProt database was chosen (75). The UniProt database relies on a much bigger database (IntAct) to highlight the protein-protein interactions with a higher number of confirmation experiments. From the 403 interactions with APP reported in IntAct, UniProt highlighted 38 main interactions with a minimum of 2 validation experiments (Table 7).

Table 7 – APP interacting proteins

PROTEIN	NUMBER OF VALIDATION EXPERIMENTS	PROTEIN	NUMBER OF VALIDATION EXPERIMENTS
APP ITSELF	104	**MED12**	2
APBA1	3	**MT-ND3**	2
APBB1	5	**NEFL**	2
APBB2	2	**NF1**	3
APLP1	2	**NGFR**	2
APLP2	2	**PCBD1**	2
APOA1	5	**PCOLCE**	3
BLMH	2	**PDIA3**	3
CALR	3	**PIN1**	2
COL18A1	2	**PRNP**	3
CTSD	2	**PSEN1**	6
FLOT1	5	**SHC1**	5
FOS	3	**SHC3**	2
GPR3	2	**SLC40A1**	5
HOMER3	3	**SPON1**	3
HSD17B10	4	**TGFB1**	3
ITM2A	3	**TGFB2**	7
JUN	2	**TNFRSF21**	3
MAP3K5	2	**TP53BP2**	3
MAPT	9		

In order to have a better visualization of the network between all the protein-protein interactions listed on the table above, a web resource (STRING) with proper characteristics was utilized. The resultant image network is seen on Figure 11.

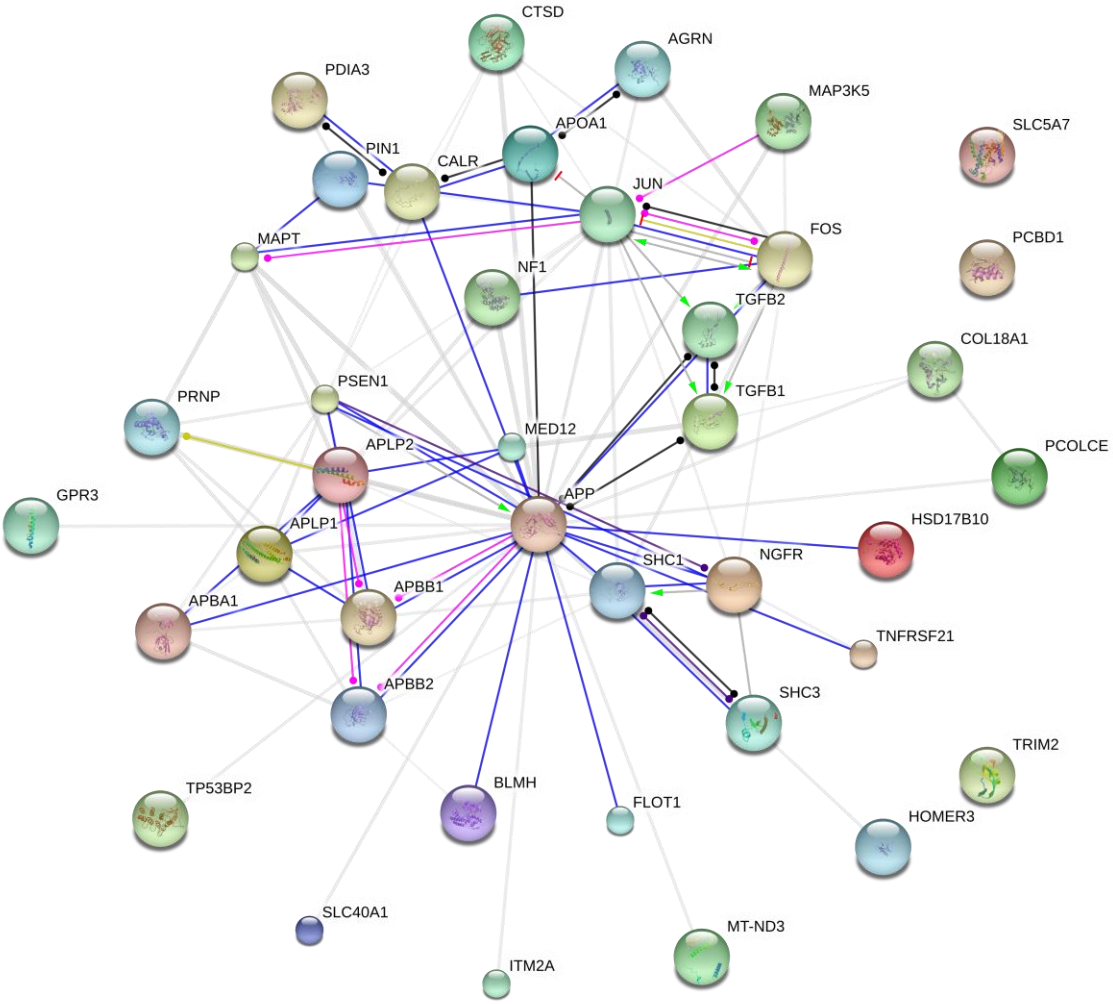

Figure 11 – Network of APP interacting proteins
The 38 APP interacting proteins are represented by circles, and thick lines correspond to interactions that are presented in the public databases. Thicker lines correspond to interactions with higher number of validated experiments.

Each protein-protein interaction has a numerical score: the higher the score, the higher the confirmation with respect to validating the interaction. On the image network obtained with STRING, that score can be analyzed by the intensity of the bands between proteins.

Using another web resource (PANTHER), the list of protein-protein interactions was analyzed to infer the relationship, function and signaling pathways of the interactions (Figure 12 and 13).

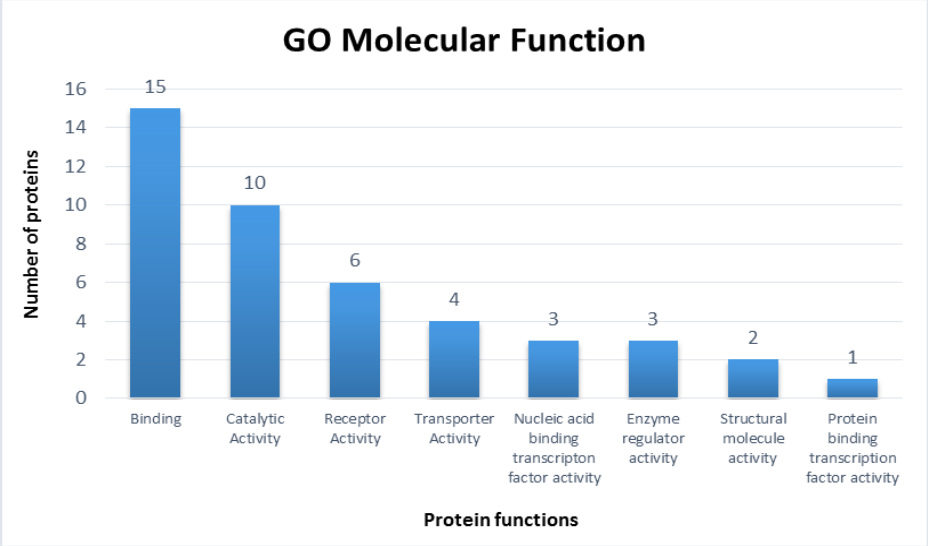

Figure 12 – Molecular functions of APP interacting proteins
The majority of APP interacting proteins have functions of binding, catalytic and receptor activity. Any APP interacting protein can have more than one function.

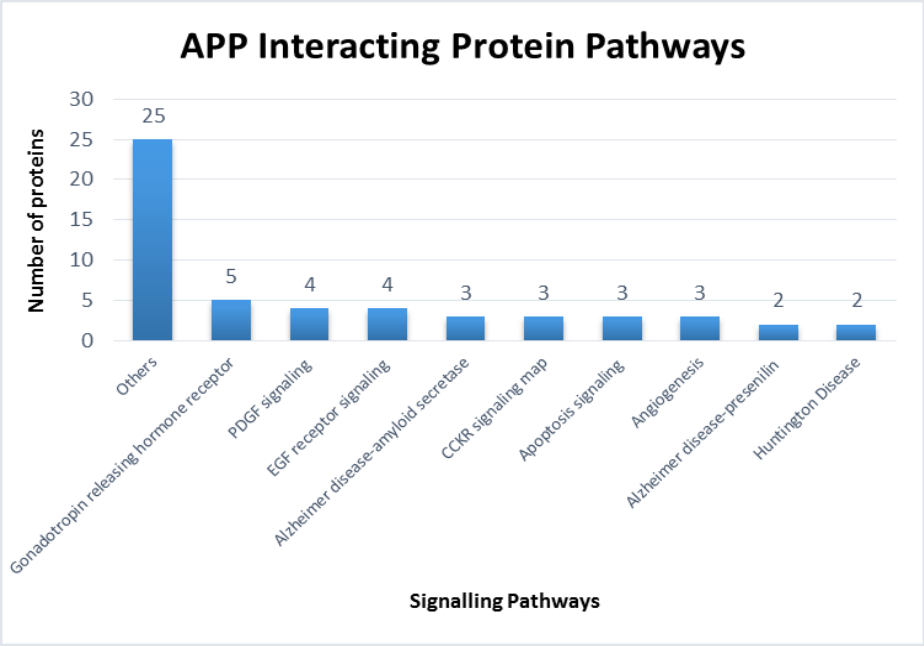

Figure 13 – Signalling pathways of APP Interacting Proteins
Several signalling pathways are represented in the figure. Of relevance to AD are the Alzheimer's Disease-amyloid secretase and the Alzheimer's disease presinilin pathways. Any APP interacting protein can have more than one signalling pathway.

Table 8 – List of APP interacting proteins and respective functions

MOLECULAR FUNCTION	NUMBER OF GENES	LIST OF PROTEINS
BINDING	15	CALR, TGFB2, JUN, TP53BP2, APBB1, APOA1, TGFB1, APP, FOS, HOMER3, MED12, PCOLCE, SHC1, APBB2, SHC3
CATALYTIC ACTIVITY	10	HSD17B10, PDIA3, NF1, APOA1, CTSD, PIN1, PSEN1, MAP3K5, PCBD1, PCOLCE
RECEPTOR ACTIVITY	6	COL18A1, GPR3, TNFRSF21, NGFR, PCOLCE
TRANSPORTER ACTIVITY	4	COL18A1, APOA1, PCOLCE
NUCLEIC ACID BINDING TRANSCRIPTION FACTOR ACTIVITY	3	JUN, FOS, MED12
ENZYME REGULATOR ACTIVITY	3	NF1, APOA1, PCOLCE
STRUCTURAL MOLECULE ACTIVITY	2	COL18A1, NEFL
PROTEIN BINDING TRANSCRIPTION FACTOR ACTIVITY	1	MED12

With the help of the bioinformatics tools (STRING, PANTHER), a lot of information can be obtained about the APP interacting proteins. The majority of the proteins that interact with APP possess catalytic or receptor activity, or are related to binding processes (Table 8). It is also observed that some APP interacting proteins are involved in signaling pathways related with Alzheimer's disease, like the Alzheimer's Disease-amyloid secretase and the Alzheimer's disease presinilin pathways (Figure 13). The other types of signaling pathways related with proteins that interact with APP shows the difficulty that is establishing a function to the APP.

So, a better understanding of APP interactions is obtained by its interactome. Studying predicted interaction networks can provide new information and future experimental research strategies. With particular interest for this thesis and future work are the proteins that interact with APP on the residues Thr668 and Tyr687 (Figure 14).

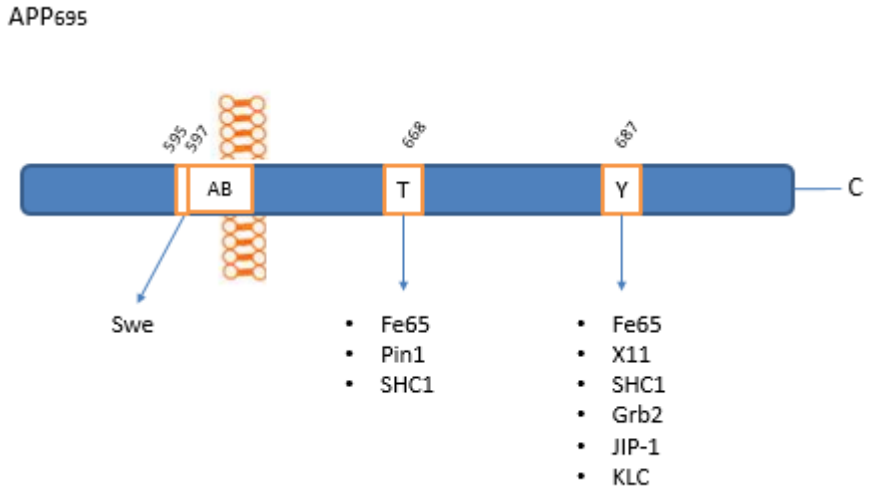

Figure 14 – Schematic representation of APP Thr668 and Tyr687 residues and proteins regulated by its phosphorylation

Phosphorylation of APP Thr668 and Tyr687 is involved in the regulation of several cell processes. When phosphorylated, APP interacts with different proteins: phosphorylation of Thr668 is shown to influence the interaction of Fe65, Pin1 and Shc1 with APP, leading to changes in APP processing; several other proteins (Fe65, X11, Shc1, Grb2, JIP-1, and KLC) interact with APP when Tyr687 is phosphorylated, modulating the metabolism and trafficking of APP .

4.2. Construction of WT and Swe Thr668 A/E APP695-GFP cDNAs

Since APP processing involves protein-protein interactions that are highly regulated by phosphorylation, the production of mutants at specific APP of phosphorylation sites, will allow us to study the role of the residues on the processing, metabolism and other physiologically relevant processes. The first step of this thesis was to construct APP Thr668 phosphomutants. The isoform used was APP695 due to its relevance in AD neuropathology.

APP Wild Type (Wt) and APP with Swedish mutation (Swe) were already available in the laboratory. The Swedish mutation is the only known APP mutation near the β-secretase cleavage site. In fact, it is a double mutation (substitution of lysine595 and methionine596 to asparagine and leucine, respectively). This mutation is known to make APP more available to BACE1, increasing the production and secretion of Aβ peptides.

Both cDNAs (Wt and Swe) were already fused with a reporter gene coding for the Green Fluorescence Protein (GFP) and inserted in a mammalian expression vector (pRc/CMV – Invitrogen) (Figure 15).

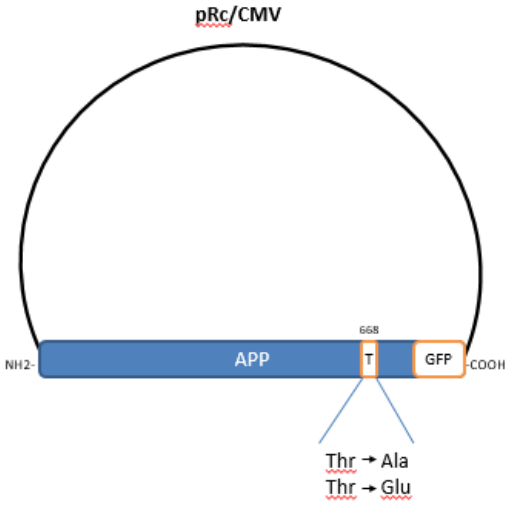

Figure 15 – Schematic representation of a mammalian expression vector with inserted APP-GFP cDNA
APP cDNAs with the specific mutations on Thr668 (Thr668 to 668A; Thr668 to 668E) were fused with a reporter gene coding for GFP and inserted into the pRc/CMV mammalian expression vector.

From these two cDNAs, 4 new phosphomutants were constructed [from Thr668 to Alanine (A) and from Thr668 to Glutamate (E)]. Alanine is a non-phosphorylatable and non-polar residue, blocking APP phosphorylation at that residue. Glutamate, on the other hand, is also a non-phosphorylatable residue, but is negatively charged, and due to its size and charge it mimics to some extent the presence of a phosphate group at that position on APP (76,77).

All the phosphomutants were produced by site directed mutagenesis PCR (QuikChange II Site-Directed Mutagenesis Kit). This *in vitro* method allows site-specific mutations in any double-stranded DNA plasmids. Following site directed mutagenesis, APP-GFP phosphomutants were amplified in bacterial systems (*E. coli* XL-1 blue competent cells) by transformation procedures. Plasmid cDNAs were extracted from the resultant bacterial cultures, and PCR products were subjected to sequential digestion with the endonucleases SmaI (produces blunt terminals) and HindIII (produces "sticky" terminals). The resultant products were resolved on a 0.5% agarose gel, extracted from the agarose gel and purified with a Gel Extration kit (QIAgen). If correctly prepared, the vector with cDNA, when digested by endonucleases, yields one band of 5.5 Kb (linearized form of the vector) and another band of around 2 Kb that corresponds to APP-GFP. For the phosphomutants cDNA plasmid, two bands of around 5.5 and 2 Kb were expected and obtained.

Subsequently, to confirm the correct mutation of the cDNAs phosphomutants, a small sample of each cDNA (80-100 ng/ul) was sent for sequencing (Lightrun Sequencing), along with 5uM of primers. The nucleotide sequences of Wt and Swe APP Thr668 point mutations were confirmed by DNA sequencing using the FinchTV software, the correct insertion of APP in the open reading frame next to the GFP coding sequence was likewise confirmed. Parts of the sequences obtained are presented in Figures 16 and 17.

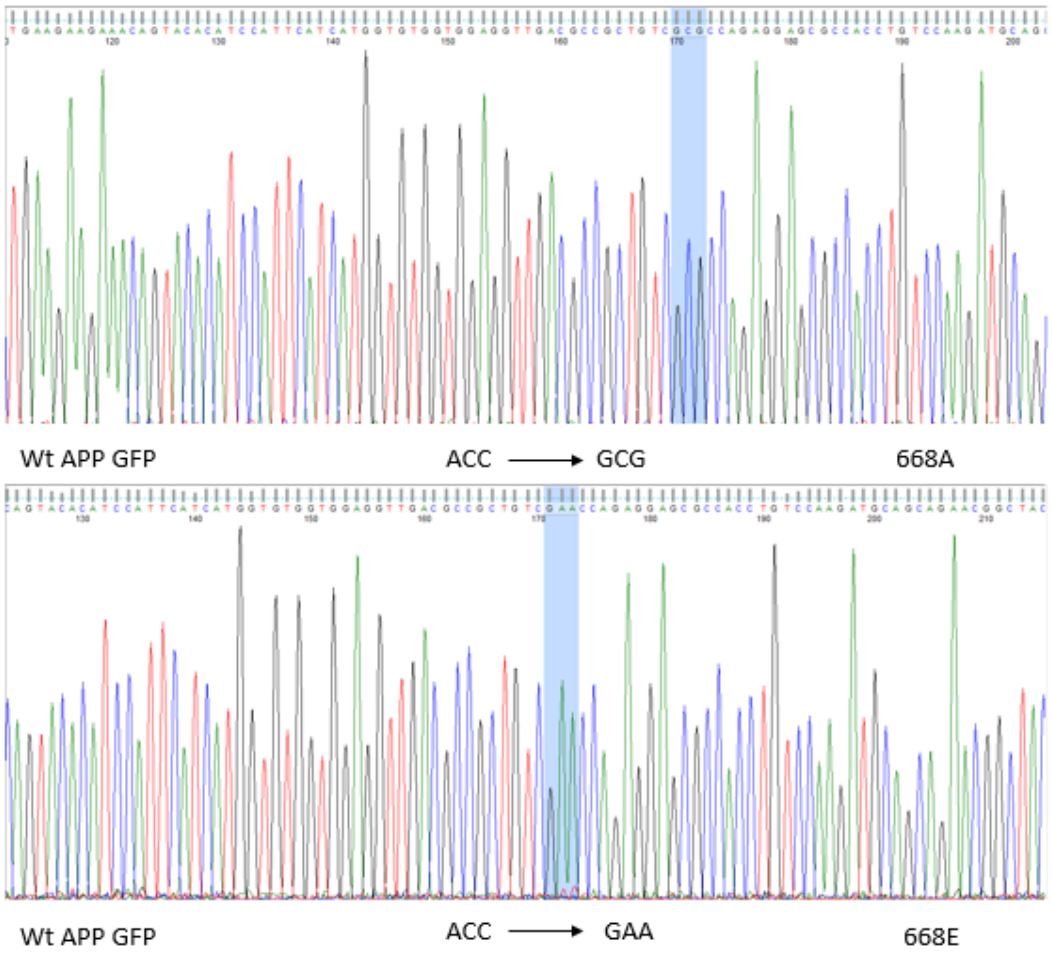

Figure 16 – Confirmation of Wt APP Thr668 mutations by DNA sequencing
From an original WT APP Thr668 cDNA, point mutations were obtained by site directed mutagenesis PCR. Threonine (ACC codon) was mutated into an Alanine (GCG codon) producing APP 668A (top). Threonine was also mutated into a Glutamate (GAA codon) producing APP668E (bottom). Images obtained with the use of FinchTV software.

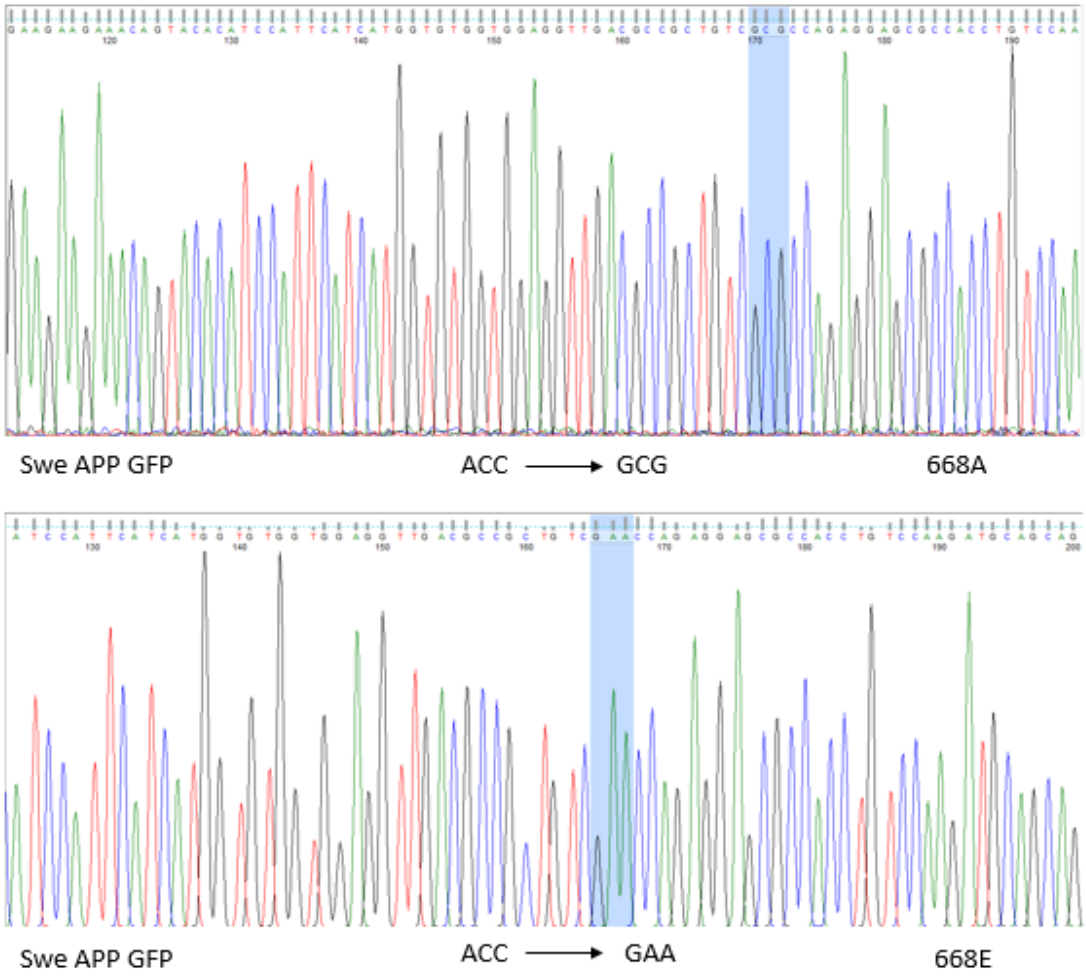

Figure 17 – Confirmation of Swe APP Thr668 mutations by DNA sequencing
From an original Swe APP Thr668 cDNA, point mutations were obtained by site directed mutagenesis PCR. Threonine (ACC codon) was mutated into an Alanine (GCG codon) producing Swe APP 668A (top). Threonine was also mutated into a Glutamate (GAA codon) producing Swe APP 668E (bottom). Images obtained with the use of FinchTV software.

APP-GFP constructs were also expressed in SH-SY5Y cells using transient transfection with Lipofectamine, and analyzed by fluorescence microscopy. All APP-GFP constructs expressed APP tagged with GFP (Figure 18).

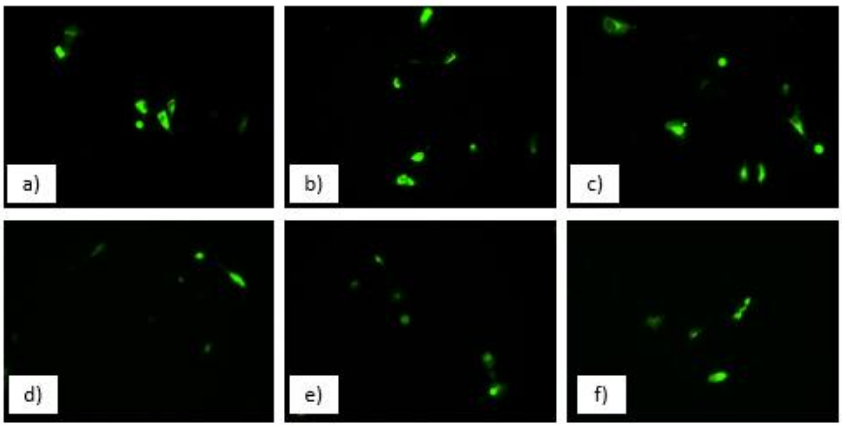

Figure 18 – Expression of APP-GFP constructs in SH-SY5Y cells
SH-SY5Y cells were transfected with the constructed APP-GFP cDNAs and its expression observed by fluorescence microscopy. All cDNA were expressed. Legend: SH-SY5Y cells transfected with a) Wt-APP Thr668; b) Wt-APP 668A; c) Wt-APP 668E; d) Swe-APP Thr668; e) Swe-APP 668A; f) Swe-APP 668E.

4.3. Optimization of the transfection method

In order to optimize SH-SY5Y cells transfection, two transient transfection methods were tested. Cells were plated in a 6-well plate, and transfected on the next day with Wt APP-GFP, Swe APP-GFP and APP T668A/E-GFP cDNAs, using the Lipofectamine method and the TurboFect TM reagent. Lipofectamine is a cationic liposome based reagent that will introduce foreign cDNA into the cells, increasing its expression. TurboFect TM is a cationic polymer that forms complexes with cDNA so that it can be integrated into the cell. Both methods are widely used in the laboratory.

The expression levels of APP-GFP from both transfection methods were evaluated first by fluorescence microscopy (Figure 19 and 20) and then by immunoblot analysis of cell lysates using the anti-APP 22C11 antibody that will bind to the N-Terminus of the APP (Figure 21).

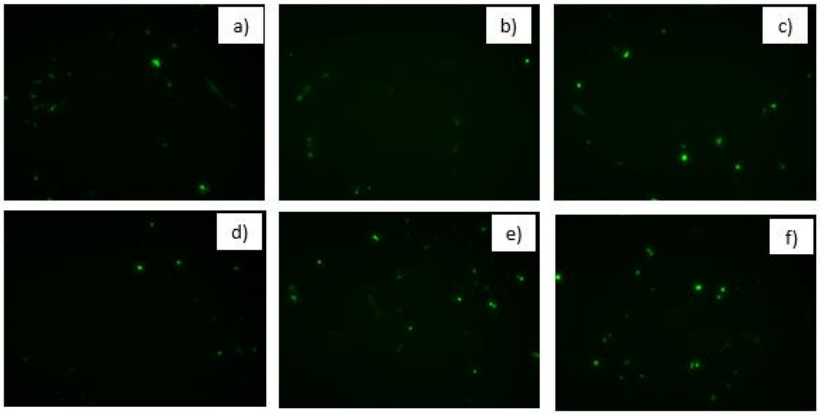

Figure 19 – Confirmation of APP-GFP constructs transfection with Lipofectamine
SH-SY5Y cells were transfected with the constructed APP-GFP cDNAs with the Lipofectamine reagent and its expression observed by fluorescence microscopy. All cDNA was expressed. Legend: SH-SY5Y cells transfected with a) Wt-APP Thr668; b) Wt-APP 668A; c) Wt-APP 668E; d) Swe-APP Thr668; e) Swe-APP 668A; f) Swe-APP 668E.

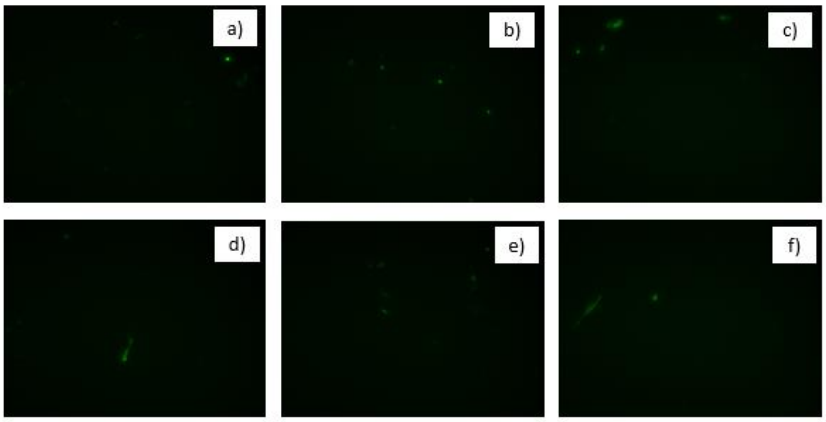

Figure 20 – Confirmation of APP-GFP constructs transfection with TurboFect TM
SH-SY5Y cells were transfected with the constructed APP-GFP cDNAs with the TurboFect TM reagent and its expression observed by fluorescence microscopy. All cDNA was expressed. Legend: SH-SY5Y cells transfected with a) Wt-APP Thr668; b) Wt-APP 668A; c) Wt-APP 668E; d) Swe-APP Thr668; e) Swe-APP 668A; f) Swe-APP 668E.

Figure 21 – Immunoblot analysis of APP-GFP transfection in SH-SY5Y cells using TurboFect and Lipofectamine
The endogenous and transfected levels of APP were visualized with the use of an anti-APP N-terminus antibody (22C11). Endogenous APP is shown by a black arrow; transfected APP-GFP is shown with a white arrow. Legend: C) Non-transfected control; Wt) Wt-APP Thr668; T668A) Wt-APP 668A; T668E) Wt-APP 668E; Swe) Swe-APP Thr668; T668A) Swe-APP 668A; T668E) Swe-APP 668E.

From the analysis of the fluorescence microscopy results, the different APP cDNAs were more expressed in SH-SY5Y cells transfected with the Lipofectamine method (Figure 19). A lower number of SH-SY5Y cells seem to be transfected with the TurboFect method (Figure 20), leading to not so good APP cDNA expression levels when compared with Lipofectamine, which have a visible higher number of transfected cells.

Lipofectamine also presents better results than TurboFect TM in the immunoblot results (Figure 21). Both endogenous (black arrow: ~110kDa) and transfected (white arrow: ~137kDa) APP levels are visible with the different transfection methods. Distinguishing between endogenous and transfected bands is possible because any GFP-tagged protein will have an increase of around 27kDa in their molecular weight, as seen with transfected APP (white arrow: ~137 kDa). However, lysates of cells transfected with Lipofectamine have a stronger transfected APP band (Figure 21, white arrow) than the TurboFect TM, showing that with the Lipofectamine method, cells were able to express more APP. This is supported by the evidence collected with fluorescence microscopy, since with Lipofectamine, more cells were transfected and higher production of APP was obtained (Figure 19 and 20). Therefore, with the collected data, the Lipofectamine method was chosen and used in all subsequent assays.

4.4. Effect of APP phosphorylation at Thr668 in Aβ production

APP is a transmembrane protein, which is regulated by phosphorylation by the action of several kinases and phosphatases. Recent studies have provided evidence of involvement of APP phosphorylation in Aβ processing (64,78). Of particular interest is the APP Thr668 residue. Phosphorylation of Thr668 at APP shows modifications of Aβ processing levels, but different studies do not reach a consensus: in some studies, Aβ processing increases (64,78); in others, the opposite results are obtained (79,80).

In order to study Aβ processing of the Wt and Swe APP Thr668 phosphomutants, SH-SY5Y cells were transfected with each cDNA and transfection was confirmed by means of fluorescence microscopy (Figure 22). Cell medium of SH-SY5Y cells transfected with APP Thr668 phosphomutants were collected. Immunoprecipitation of Aβ peptides on collected cell medium samples was prepared, and were subsequently analyzed by Aβ-SDS-PAGE in the presence of 8M urea. Cell medium of cells non-transfected and of cells transfected only with an empty GFP-vector were also collected, immunoprecipitated and loaded in the gel as controls (Figure 23).

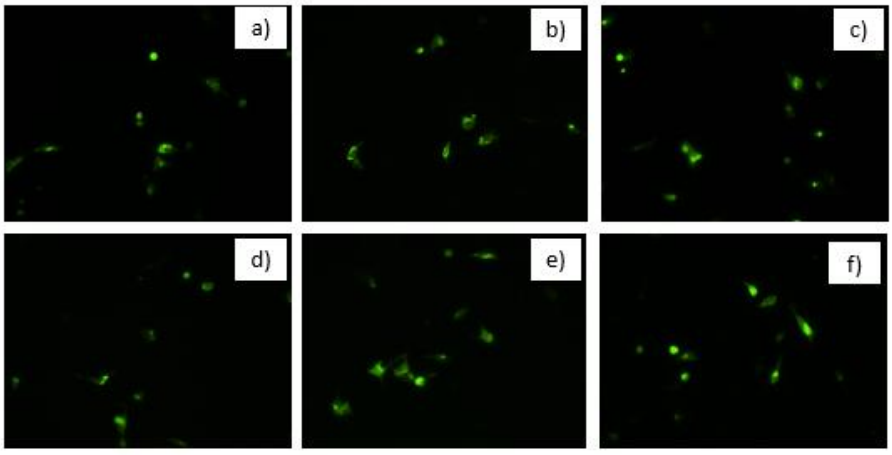

Figure 22 – Confirmation of APP-GFP phosphomutants transfection with Lipofectamine
SH-SY5Y cells were transfected with the APP-GFP phosphomutants cDNAs using the Lipofectamine reagent and its expression was observed by fluorescence microscopy. All cDNA was expressed. Legend: SH-SY5Y cells transfected with a) Wt-APP Thr668; b) Wt-APP 668A; c) Wt-APP 668E; d) Swe-APP Thr668; e) Swe-APP 668A; f) Swe-APP 668E.

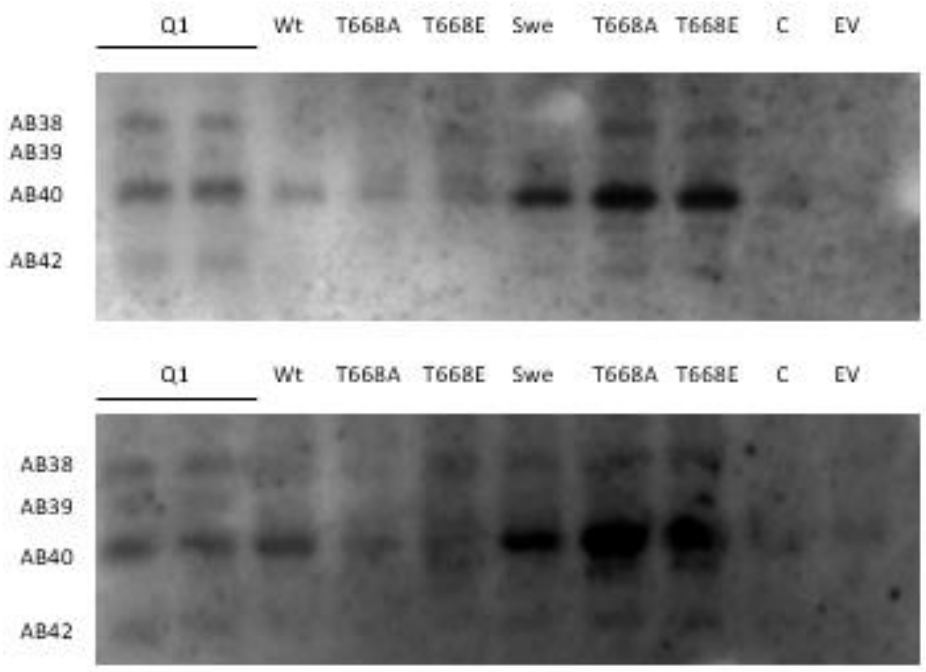

Figure 23 – Aβ production of APP-GFP phosphomutant visualized by Aβ-SDS-PAGE
SH-SY5Y cell medium were immunoprecipitated to collect Aβ and then analysed by Aβ-SDS-PAGE. Q1 mix with synthetic Aβ peptides (Aβ 1-37, Aβ 1-38, Aβ 1-39, Aβ 1-40 and Aβ 1-42) were used as control. The top and the bottom image show two obtained results. Legend: Q1) Mix of synthetic of Aβ peptides; Wt) Wt-APP Thr668; T668A) Wt-APP 668A; T668E) Wt-APP 668E; Swe) Swe-APP Thr668; T668A) Swe-APP 668A; T668E) Swe-APP 668E; C) Non-transfected control; EV) Empty-GFP vector control.

Using the conventional SDS-PAGE system, different Aβ peptides would migrate as a single band (4kDa). The presence of urea on the Aβ-SDS-PAGE, will prevent Aβ aggregation and induce Aβ specific conformational changes, affecting their molecular radii. Thus, Aβ peptides (4kDa) with differences in one or two amino-acids that would migrate in a single band in a SDS-PAGE, can be easily separated and visualized into different bands (Figure 23) (68–70).

A mixture of Aβ synthetic peptides (Q1 mix: Aβ 1-37, Aβ 1-38, Aβ 1-39, Aβ 1-40 and Aβ 1-42) is used as control, mimicking the different Aβ peptides ratio in the human body (Table 9). On the Aβ-SDS-PAGE, the bigger Aβ peptides run for a longer time than the shorter Aβ peptides, not obeying the law of mobility/molecular weight relationship that is observed on SDS-PAGE.

Table 9 – Q1 mix of Synthetic Aβ peptides

Aβ-peptide	*Q1 mix (pg)*
1-37	30
1-38	60
1-39	30
1-40	120
1-42	60

With the use of fluorescence microscopy, SH-SY5Y cells were shown to visually express the transfected APP-cDNAs (Figure 22). Using Aβ-C-terminal antibody (6E10) to the cell medium samples, one expects to see the Aβ production for the different phosphomutants. All phosphomutants and controls produced Aβ peptides, and more than one Aβ band was evident for each APP 668A/E phosphomutant (Figure 23). As anticipated, according to the literature, Aβ1-40 was the main Aβ peptide produced by all transfected and non-transfected cells (Figure 23). Other weaker bands are also observed, especially for the Swe APP 668A/E phosphomutants: one corresponding to Aβ1-38 and another equivalent to Aβ1-42. The results followed the estimated Aβ distribution:

$$A\beta 1\text{-}40 > A\beta 1\text{-}42 = A\beta 1\text{-}38$$

As expected, the Swe APP 668A/E phosphomutants seem to produce more Aβ than normal. Aβ1-40 is the major produced Aβ peptide, but even Aβ1-38 and 1-42 appear to be produced in higher quantities (Figure 23). Swedish mutation of APP was proposed to make APP more favorable to be cleaved by BACE1, leading to higher amounts of total Aβ peptides, although keeping the Aβ1-40/Aβ1-42 ratio (81,82). A small increase of Aβ production appears to happen on the Swe APP 668A (non-phosphorylated state) in comparison with Swe APP 668E (Figure 23), although more studies and quantitative analysis have to carried out to further validate this conclusion.

Regarding Wt APP and its 668A/E phosphomutants, Aβ production also seems to be increased when compared with non-transfected controls (Figure 23). Available literature does not reach a consensus about the effect of Thr668 phosphorylation on Aβ production.

Some report an increase in Aβ production (53,58), while others report a decrease or do not observe a connection between APP Thr668 phosphorylation and Aβ production (79,80). However, we show that the mimic of phosphorylated state of Wt APP Thr668 (668E) seems to produce higher levels of Aβ peptides (Aβ1-40 and Aβ1-38) (Figure 23, bottom). Again, more studies and quantitative analysis should be carried out so that this conclusion can be fully embraced.

Quantitative comparisons between phosphomutants were not possible due immunoprecipitation not being a quantitative method. One way to solve this problem would be to run at the same time a SDS-PAGE with the lysates of cells used for the Aβ-SDS-PAGE. This way, we would have a notion with respect to the total APP levels (endogenous plus transfected), and with that information we could extrapolate the transfected levels of each phosphomutant and infer a quantitative analysis of Aβ production.

4.5. Effect of APP phosphorylation at Thr668 in CTF formation

Many different cleavage sites have been identified in APP. Both β- and γ-secretases may cleave APP at multiple sites. Considering that phosphorylation of APP Thr668 is supposedly involved in an increased processing by BACE1, one would expect intracellular βCTF to be higher for APP Thr668 phosphomutants.

To test this hypothesis, SH-SY5Y cells were transfected with Wt APP Thr668 and Wt APP 668A/E phosphomutants. Transfection was conducted for 48h in order to allow the cells to express the phosphomutants. Non-transfected SH-SY5Y cells were used as a control, as well as cells transfected with an empty GFP Vector. Transfection was confirmed by fluorescence microscopy (Figure 24). Cell lysis was later achieved by addition of SDS 1%, and cell lysate samples were quantified and then loaded on a 5%-20% denaturing SDS-PAGE (Figure 25)

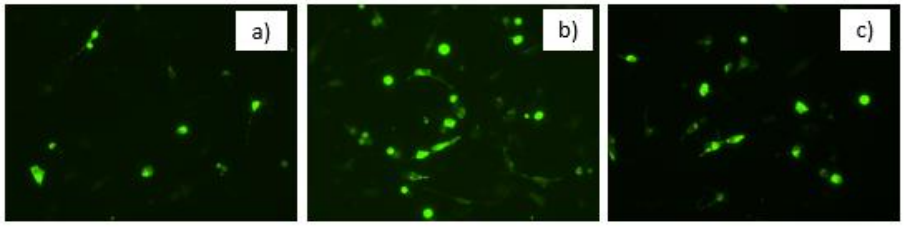

Figure 24 – Confirmation of APP-GFP phosphomutants transfection with Lipofectamine
SH-SY5Y cells were transfected with the APP-GFP phosphomutants cDNAs using the Lipofectamine reagent and its expression was observed by fluorescence microscopy. All cDNA was expressed. Legend: SH-SY5Y cells transfected with a) Wt-APP Thr668; b) Wt-APP 668A; c) Wt-APP 668E.

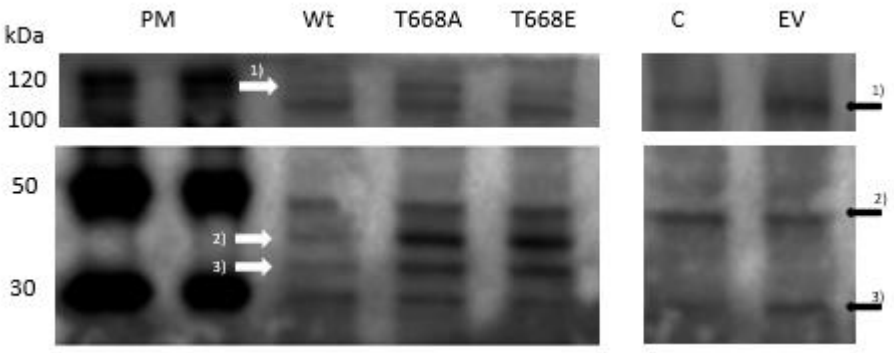

Figure 25 – Immunoblot analysis of CTF formation of Wt APP-GFP phosphomutants
SH-SY5Y cells were transfected with Wt APP-GFP phosphomutants and cell lysates were collected and run on a denaturing SDS-PAGE. APP C-terminal antibody was used. Endogenous APP (black arrow 1) and its endogenous fragments (black arrows 2 and 3) are presented. Transfected APP-GFP (white arrow 1) and β- (white arrow 2) and α CTF-GFP (white arrow 3) are also visible. Legend: PM) Protein Marker; Wt) Wt-APP Thr668; T668A) Wt-APP 668A; T668E) Wt-APP 668E; C) Non-transfected Control; EV) Empty-GFP vector control.

Western blot analysis with APP C-terminal antibody revealed, as expected, the SH-SY5Y endogenous APP [black arrow 1) ~110kDa] and several endogenous APP fragments [black arrows 3) and 2) ~30 and ~50 kDa] on both controls and Wt APP-GFP phosphomutants (Figure 25). Three extra bands, migrating at ~120 kDa (white arrow 1), ~40 kDa (white arrow 2) and ~35 kDa (white arrow 3) appear only in the APP-GFP transfected cellular lysates, and not in the controls (Figure 25). These are likely to correspond to APP-GFP (white arrow 1 ~137 kDa) and to β (white arrow 2 ~39 kDa) and α CTF-GFP (white arrow 3 ~35 kDa). As expected, differences between phosphomutants and controls are visible. Any GFP-tagged protein will have an increase of around 27kDa in their molecular weight, and this is visualized in the Figure 25 (white arrows 1,2 and 3).

In essence, both Wt APP Thr668A and 668E seem to present stronger levels of α and β CTF-GFP (Figure 25, white arrows 2 and 3). It is also observed that more βCTF-GFP is produced when compared to α-CTF-GFP, but quantitative analysis and more studies are required. Literature supports that β-CTFs generated by BACE1 are preferentially phosphorylated on Thr668 over the α-CTFs, and that CTFs of Thr668 phosphorylated APP are elevated in AD brains (78). Our results seem to propose that mimic of both phosphorylated (668E) and non-phosphorylated state (668A) of Wt APP Thr668 can regulate the β-secretase processing of APP, increasing the levels of βCTF (Figure 25, white arrow 2).

4.6. Immunocytochemistry of the APP/Fe65/PP1γ trimeric complex in SH-SY5Y cells

A clear relationship between APP, Fe65 and PP1γ was shown on a previous study (84). Fe65 is the bridging protein between APP and PP1γ, forming the trimeric complex APP/Fe65/PP1γ. The phosphorylation of Thr668 was also shown to be a regulatory process of the trimeric complex. When phosphorylated by PP1γ on Thr668, APP is made available for the subsequent processing events (84). Co-localization of the trimeric complex was found in the cell and nuclear membrane, but the three proteins are also described to be found in the nucleus (84).

In order to visualize *in vivo* whether the APP/Fe65/PP1γ trimeric complex was present in SH-SY5Y cells transfected with 668A/E mutants, we decided to perform an immunocytochemistry and observe the co-localization of APP phosphomutants, Fe65 and PP1γ.

The following images (Figure 26 and 27) represent the results obtained.

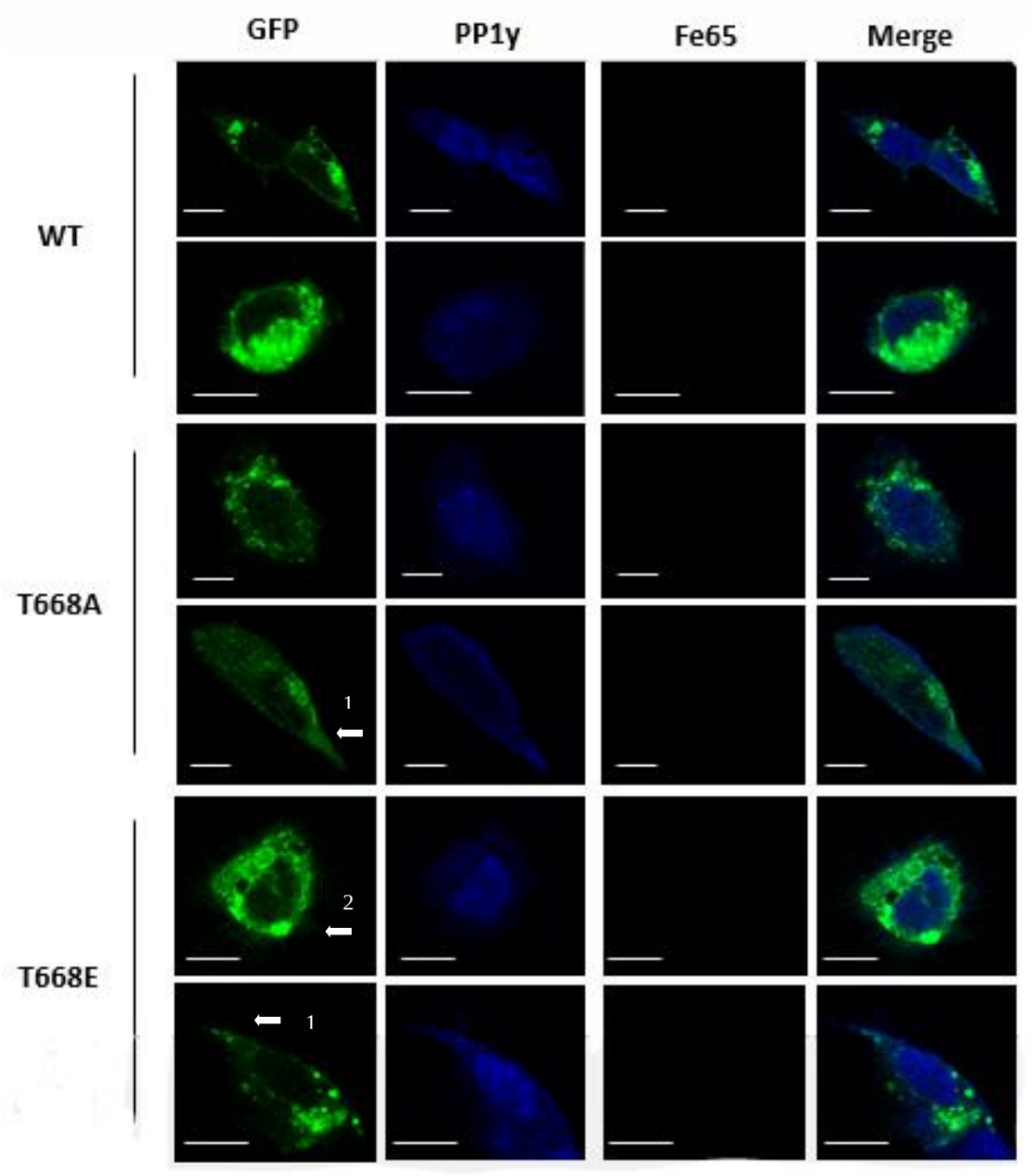

Figure 26 – PP1 gamma, Fe65 and Wt APP phosphomutants (668A/E) co-localization in SH-SY5Y cells

Wt APP-GFP phosphomutants (668A/E) appears as green, PP1 gamma as blue and Fe65 as red. Merge represent the co-localization image of all the 3 marked proteins. White arrow 1 represent neuronal growth cones, while white arrow 2 represent filopodia. The image scale is 10 um. Legend: Wt) Wt-APP Thr668; T668A) Wt-APP 668A; T668E) Wt-APP 668E.

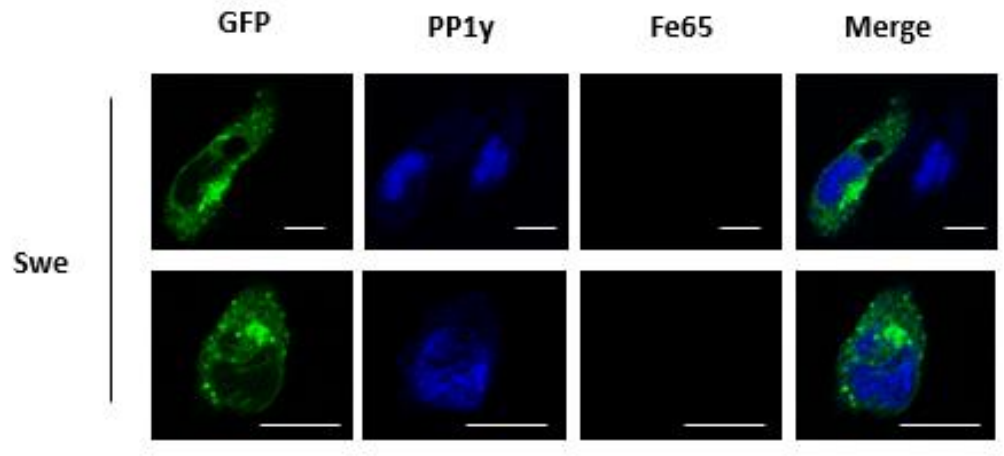

Figure 27 – PP1 gamma, Fe65 and Swe APP phosphomutants (668A/E) co-localization in SH-SY5Y cells

Swe APP-GFP appears as green, PP1 gamma as blue and Fe65 as red. Merge represent the co-localization image of all the 3 marked proteins. The image scale is 10 um. Legend: Swe) Swe APP Thr668.

By analyzing the above figures (Figure 26 and 27), it is possible to observe that only Fe65 (marked as red) did not show any kind of signal. That is explained by the fact that the available anti-Fe65 antibody was old and not working properly. A new anti-Fe65 antibody has to be used to prove the presence of the APP/Fe65/PP1γ trimeric complex on cells transfected with APP 668A/E phosphomutants.

Nonetheless, both APP phosphomutants (marked as green) and PP1γ (marked as blue) show a perceptible signal in all the obtained images (Figure 26 and 27). It is possible to see that APP is found on the cell membrane, Golgi apparatus and endocytic vesicles, subcellular neuronal sites known to have higher concentrations of APP (Figure 26 and 27). In neurons, PP1γ is highly concentrated on dendritic spines and presynaptic terminals. Those subcellular locations are not visible with undifferentiated SH-SY5Y cells. However, PP1γ also shows expression in the nucleus (nucleolus and nucleoplasm) and in the cytoplasm, with exchanges between those cellular compartmens. It is possible to see on the obtained images (Figure 26 and 27) that PP1γ is easily found on the nucleus and also spread throught the cytoplasm.

APP Thr668 phosphorylation is described as an event that will lead to the differentiation of neuronal cells, proved by the presence of APP in neurites and growth cones. Both cells transfected with APP Wt 668A/E (Figure 26) present some morfological

changes related to phosphorylation events on Thr668. On the images obtained, it is possible to see the appearance of growth cones (Figure 26, white arrow 1), as well as the presence of some filopodia (Figure 26, white arrow 2). Both Wt and Swe APP Thr668 transfected SH-SY5Y cells present the normal morphology associated with the cell type: epithelial-like cells with polygonal and regular shapes and without axons and neurites (Figure 26 and 27, Wt and Swe).

Unfortunately, both Swe 668A/E phosphomutants (marked as green) did not show any signal, and so, both PP1γ and Fe65 were also not obtained. It is critical to repeat the experiment with the Swe 668A/E phosphomutants so that new information can be acquired.

Nevertheless, the experimental procedure here performed represent a preliminary study that needs to be optimized and repeated in order to confirm the physical interactions between APP 668A/E phosphomutants and Fe65 and PP1γ. No co-localization analysis was made between APP and PP1γ since the number of transfected cells was low.

5. Concluding Remarks and Future Prospects

Phosphorylation plays an important role in all cellular functions, and is highly associated with APP and with AD. Several studies imply an important role of APP Thr668 in the development of AD, especially on APP metabolism. Recent studies also show that phosphorylation of this residue is needed to form trimeric complexes that are involved in Aβ production. According to the results obtained in this thesis, and with the use of the constructed Thr668 phosphomutants (668A/E), we show that APP metabolism seems to be related to phosphorylation on APP Thr668. There is a clear increase in Aβ production of Swe APP phosphomutants (668A/E), being that Aβ1-40 is the major Aβ species produced, followed by Aβ1-38 and Aβ1-42 (Figure 23). Wt APP phosphomutants (668A/E) also show some increase in Aβ production (Figure 23), as well as higher levels of β-CTF (Figure 25). However, more studies have to be carried out, as well as quantitative analysis of the visible bands. Preliminary co-localization studies of the APP/Fe65/PP1γ trimeric complex have shown the subcellular localization of Wt APP phosphomutants and PP1γ. More studies have to be realized in order to obtain a proper co-localization of the three proteins that form the trimeric complex.

With this thesis, important tools (APP Interactome, APP phosphomutants, Aβ-SDS-PAGE, Immunocytochemistry) were developed that will certainly help to prove the initially proposed hypothesis.

So, in future studies, it would be of high importance to continue to study the co-localization of different protein and complexes that were proved, by the APP Interactome to interact with APP, especially on the Thr668 residue. Of particular interest are both Fe65/PP1γ and Shc/Grb2 complexes. The first one was proved to be interacting with Wt APP-Thr668, and initial studies with APP phosphomutants were executed, but more are needed; the second complex has not yet been studied with regard to phosphorylation of APP Thr668.

Other phosphorylated residues can be studied with the developed tools, with particular interest the Tyr687 residue on APP, since it is a residue with a high number of interacting proteins.

It would also be interesting to optimize transfection conditions with other cell lines, like CHO or HeLa, so that a more reproducible and reliable transfection method is

achieved. In order to avoid the usual problems concerning transient transfection, it would be of interest to develop stable cell lines with the produced phosphomutants. This way, new additional information could also be obtained.

Although not discussed in the scope of this thesis, subcellular localization is fundamental for determining APP processing, its cleavages and the peptide fragments produced. Namely Aβ production has been intrinsically associated with cleavages that occur at lipid reach sites (lipid rafts) in the plasma membrane. Nonetheless, preliminary studies were realized with depletion of cholesterol from the lipid rafts (data not shown). In the future, it will be interesting to study APP phosphomutants processing without the presence of lipid rafts (by cholesterol depletion using Methyl-β Cyclodextrin). From a neuropathological standpoint, this is particularly relevant as diseases as diabetes, for instance, have been associated with the onset of AD.

6. References

1. Han X, Rozen S, Boyle SH, Hellegers C, Cheng H, Burke JR, et al. Metabolomics in early Alzheimer's disease: Identification of altered plasma sphingolipidome using shotgun lipidomics. PLoS One. 2011.

2. Association A. 2014 Alzheimer's Disease Facts and Figures. Alzheimer's Dement. 2014. Available from: https://www.alz.org/downloads/facts_figures_2014.pdf

3. Ortiz GG, Pacheco-moisés FP, Flores-alvarado LJ, Macías-islas M a, Velázquez-brizuela IE, Ramírez-anguiano AC, et al. Alzheimer Disease and Metabolism : Role of Cholesterol and Membrane Fluidity. Understanding Alzheimer's Disease. 2013.

4. Tarawneh R, Holtzman DM. The clinical problem of symptomatic Alzheimer disease and mild cognitive impairment. Cold Spring Harb Perspect Med. 2012.

5. Castellani RJ, Rolston RK, Smith M a. Alzheimer Disease. Dis a Mon. 2011.

6. Holtzman DM, Herz J, Bu G. Apolipoprotein E and apolipoprotein receptors: normal biology and roles in Alzheimer's disease. Cold Spring Harb Perspect Med. 2012.

7. Paolo G Di, Kim T. Linking Lipids to Alzheimer ' s Disease : Cholesterol and Beyond. Aging (Albany NY). 2012.

8. Bamburg JR, Bloom GS. Cytoskeletal Pathologies of Alzheimer Disease. Cell Motil Cytoskelet. 2009.

9. Zhao Y, Zhao B. Oxidative Stress and the Pathogenesis of Alzheimer's Disease. Oxid Med Cell Longev. 2013.

10. Kumar A, Singh A, Ekavali. A review on Alzheimer's disease pathophysiology and its management: an update. Pharmacol Reports. 2015.

11. Cheng H, Vetrivel KS, Gong P, Parent A, Thinakaran G. Mechanisms of Disease: new therapeutic strategies for Alzheimer's disease—targeting amyloid precursor protein processing in lipid rafts. Nat Clin Pract Neurol. 2007.

12. Rojo L, Sjöberg M, Hernández P, Zambrano C, Maccioni R. Roles of cholesterol

and lipids in the etiopathogenesis of alzheimer's disease. J Biomed Biotechnol. 2006.

13. Burns M, Rebeck GW. Intracellular Cholesterol Homeostasis and Amyloid Precursor Protein Processing. Biochim Biophys Acta. 2010.

14. Rushworth J V, Hooper NM. Lipid Rafts: Linking Alzheimer's Amyloid-β Production, Aggregation, and Toxicity at Neuronal Membranes. Int J Alzheimers Dis. 2010.

15. Haass C. Take five--BACE and the gamma-secretase quartet conduct Alzheimer's amyloid beta-peptide generation. EMBO J. 2004.

16. Cerasoli E, Ryadnov MG, Austen BM. The elusive nature and diagnostics of misfolded Aβ oligomers. Front Chem. 2015.

17. Tu S, Okamoto S, Lipton SA, Xu H. Oligomeric Aβ-induced synaptic dysfunction in Alzheimer's disease. Mol Neurodegener. 2014.

18. Reiss AB, Voloshyna I. Regulation of Cerebral Cholesterol Metabolism in Alzheimer's Disease. J Investig Med. 2012.

19. Iqbal K, Bolognin S, Wang X, Basurto-Islas G, Blanchard J, Tung YC. Animal models of the sporadic form of Alzheimer's disease: focus on the disease and not just the lesions. J Alzheimers Dis. 2013.

20. Wong BX, Hung YH, Bush AI, Duce J a. Metals and cholesterol: Two sides of the same coin in Alzheimer's disease pathology. Front Aging Neurosci. 2014.

21. Walter J, van Echten-Deckert G. Cross-talk of membrane lipids and Alzheimer-related proteins. Mol Neurodegener. Molecular Neurodegeneration; 2013.

22. Olgiati P, Politis AM, Papadimitriou GN, De Ronchi D, Serretti A. Genetics of late-onset Alzheimer's disease: update from the alzgene database and analysis of shared pathways. Int J Alzheimers Dis. 2011.

23. O'Brien R, Wong P. Amyloid precursor protein processing and alzheimer's disease. Annu Rev Neurosci. 2011.

24. Mayeux R, Stern Y. Epidemiology of Alzheimer disease. Cold Spring Harb Perspect

Med. 2012.

25. Reitz C, Mayeux R. Alzheimer disease: epidemiology, diagnostic criteria, risk factors and biomarkers. Biochem Pharmacol. 2014.

26. Mattson MP. Pathways Towards and Away from Alzheimer's Disease. Nature. 2004.

27. Tanzi RE. The genetics of Alzheimer disease. Cold Spring Harb Perspect Med. 2012.

28. Liu C-C, Kanekiyo T, Xu H, Bu G. Apolipoprotein E and Alzheimer disease: risk, mechanisms and therapy. Nat Rev Neurol. Nature Publishing Group; 2013.

29. Bu G. Apolipoprotein E and its receptors in Alzheimer's disease: pathways, pathogenesis and therapy. Nat Rev Neurosci. 2009.

30. Holtzman DM, Morris JC, Goate AM. Alzheimer ' s Disease : The Challenge of the Second Century. Sci Transl Med. 2011.

31. Adibhatla RM, Hatcher JF. Altered Lipid Metabolism in Brain Injury and Disorders. Subcell Biochem. 2014.

32. Hannaoui S, Shim S, Cheng Y, Corda E, Gilch S. Cholesterol Balance in Prion Diseases and Alzheimer's Disease. Viruses. 2014.

33. Florent-Béchard S, Desbène C, Garcia P, Allouche A, Youssef I, Escanyé MC, et al. The essential role of lipids in Alzheimer's disease. Biochimie. 2009.

34. Grimm MOW, Zimmer VC, Lehmann J, Grimm HS, Hartmann T. The impact of cholesterol, DHA, and sphingolipids on alzheimer's disease. Biomed Res Int. 2013.

35. Simons K, Ehehalt R. Cholesterol, lipid rafts, and disease. J Clin Invest. 2002.

36. Shim YS, Morris JC. Biomarkers predicting Alzheimer's disease in cognitively normal aging. J Clin Neurol. 2011.

37. Anoop A, Singh PK, Jacob RS, Maji SK. CSF Biomarkers for Alzheimer's Disease Diagnosis. Int J Alzheimers Dis. 2010.

38. Walhovd KB, Fjell AM, Brewer J, McEvoy LK, Fennema-Notestine C, Hagler DJ, et al. Combining MR imaging, positron-emission tomography, and CSF biomarkers in the diagnosis and prognosis of Alzheimer disease. AJNR Am J Neuroradiol. 2010.

39. Serrano-Pozo A, Frosch MP, Masliah E, Hyman BT. Neuropathological alterations in Alzheimer disease. Cold Spring Harb Perspect Med. 2011.

40. Lleó A, Greenberg SM, Growdon JH. Current pharmacotherapy for Alzheimer's disease. Annu Rev Med. Annual Reviews; 2006.

41. Zhou Z-D, Chan CH-S, Ma Q-H, Xu X-H, Xiao Z-C, Tan E-K. The roles of amyloid precursor protein (APP) in neurogenesis: Implications to pathogenesis and therapy of Alzheimer disease. Cell Adh Migr. 2011.

42. Haass C, Kaether C, Thinakaran G, Sisodia S. Trafficking and proteolytic processing of APP. Cold Spring Harb Perspect Med. 2012.

43. Zhang Y, Thompson R, Zhang H, Xu H. APP processing in Alzheimer's disease. Mol Brain. BioMed Central Ltd; 2011.

44. Hicks D a., Nalivaeva NN, Turner AJ. Lipid rafts and Alzheimer's disease: Protein-lipid interactions and perturbation of signaling. Front Physiol. 2012.

45. Da Cruz e Silva EF, Da Cruz e Silva O a B. Protein phosphorylation and APP metabolism. Neurochem Res. 2003.

46. Zhang H, Ma Q, Zhang Y, Xu H. Proteolytic processing of Alzheimer's β-amyloid precursor protein. J Neurochem. 2012.

47. Korade Z, Kenworthy AK. Lipid rafts, cholesterol, and the brain. Neuropharmacology. 2008.

48. Malchiodi-Albedi F, Paradisi S, Matteucci A, Frank C, Diociaiuti M. Amyloid oligomer neurotoxicity, calcium dysregulation, and lipid rafts. Int J Alzheimers Dis. 2011.

49. Haughey NJ. Sphingolipids in Neurodegeneration. NeuroMolecular Med. 2010.

50. Pike LJ. The challenge of lipid rafts. J Lipid Res. 2009.

51. Sengupta P, Baird B, Holowka D. Lipid rafts, fluid/fluid phase separation, and their relevance to plasma membrane structure and function. Semin Cell Dev Biol. 2007.

52. Waheed AA, Freed EO. Lipids and Membrane Microdomains in HIV-1 Replication. Virus Res. 2009.

53. George KS, Wu S. Lipid Raft: A Floating Island Of Death or Survival. Toxicol Appl Pharmacol. 2012.

54. de Laurentiis A, Donovan L, Arcaro A. Lipid rafts and caveolae in signaling by growth factor receptors. Open Biochem J. 2007.

55. Bieberich E. It's a lipid's world: Bioactive lipid metabolism and signaling in neural stem cell differentiation. Neurochem Res. 2012.

56. El-Sayed A, Harashima H. Endocytosis of gene delivery vectors: from clathrin-dependent to lipid raft-mediated endocytosis. Mol Ther. 2013.

57. Marzolo M-P, Bu G. Lipoprotein receptors and cholesterol in APP trafficking and proteolytic processing, implications for Alzheimer's disease. Changes. 2012.

58. Cole SL, Vassar R. The role of amyloid precursor protein processing by BACE1, the β-secretase, in Alzheimer disease pathophysiology. J Biol Chem. 2008.

59. Ehehalt R, Keller P, Haass C, Thiele C, Simons K. Amyloidogenic processing of the Alzheimer β-amyloid precursor protein depends on lipid rafts. J Cell Biol. 2003.

60. Venugopal C, Demos CM, Rao KSJ, Pappolla MA, Sambamurti K. Beta-secretase: Structure, Function, and Evolution. CNS Neurol Disord - Drug Targets. 2008.

61. Luo X, Yan R. Inhibition of BACE1 for therapeutic usein Alzheimer's disease. Int J Clin Exp Pathol. 2010.

62. Rebelo S, Vieira SI, Esselmann H, Wiltfang J, Da Cruz E Silva EF, Da Cruz E Silva O a B. Tyrosine 687 phosphorylated Alzheimer's amyloid precursor protein is retained intracellularly and exhibits a decreased turnover rate. Neurodegener Dis. 2007.

63. Chang K-A, Kim H-S, Ha T-Y, Ha J-W, Shin KY, Jeong YH, et al. Phosphorylation of amyloid precursor protein (APP) at Thr668 regulates the nuclear translocation of the APP intracellular domain and induces neurodegeneration. Mol Cell Biol. 2006.

64. Chang K-A, Kim H-S, Ha T-Y, Ha J-W, Shin KY, Jeong YH, et al. Phosphorylation of amyloid precursor protein (APP) at Thr668 regulates the nuclear translocation of the APP intracellular domain and induces neurodegeneration. Mol Cell Biol. 2006.

65. Da Cruz E Silva O a B, Fardilha M, Henriques AG, Rebelo S, Vieira S, Da Cruz E Silva EF. Signal Transduction Therapeutics. J Mol Neurosci. 2004.

66. Kovalevich J, Langford D, Kovalevich J, Langford D. Considerations for the Use of SH-SY5Y Neuroblastoma Cells in Neurobiology. METHODS Mol Biol. 2013.

67. GE Healthcare. Western blotting: Principles and Methods. 2014. 1-181 p.

68. Wiltfang J, Smirnov a, Schnierstein B, Kelemen G, Matthies U, Klafki HW, et al. Improved electrophoretic separation and immunoblotting of beta-amyloid (A beta) peptides 1-40, 1-42, and 1-43. Electrophoresis. 1997.

69. Wiltfang J, Esselmann H, Bibl M, Smirnov A, Otto M, Paul S, et al. Highly conserved and disease-specific patterns of carboxyterminally truncated Abeta peptides 1-37/38/39 in addition to 1-40/42 in Alzheimer's disease and in patients with chronic neuroinflammation. J Neurochem. 2002.

70. Wiltfang J, Staufenbiel M. Electrophoretic Separation of BetaA4 peptides (1-40) and (1-42). 1996.

71. Burry RW. Immunocytochemistry - A Practical Guide for Biomedical Research . Springer New York; 2010.

72. Vidal M, Cusick ME, Barabási A-L. Interactome networks and human disease. Cell. 2011.

73. Garcia-Alonso L, Jiménez-Almazán J, Carbonell-Caballero J, Vela-Boza A, Santoyo-López J, Antiñolo G, et al. The role of the interactome in the maintenance of deleterious variability in human populations. Mol Syst Biol. 2014.

74. Musungu B, Bhatnagar D, Brown RL, Fakhoury AM, Geisler M. A predicted protein interactome identifies conserved global networks and disease resistance

subnetworks in maize. Front Genet. 2015.

75. APP - Amyloid beta A4 protein precursor - Homo sapiens (Human) - APP gene & protein. Available from: http://www.uniprot.org/uniprot/P05067

76. da Cruz E Silva O a B, Vieira SI, Rebelo S, da Cruz e Silva EF. A model system to study intracellular trafficking and processing of the Alzheimer's amyloid precursor protein. Neurodegener Dis. 2004.

77. Paz SIMPVG e. Phosphorylation-dependent Alzheimer's Amyloid Precursor Protein (APP) Targeting. 2006.

78. Lee M-S, Kao S-C, Lemere CA, Xia W, Tseng H-C, Zhou Y, et al. APP processing is regulated by cytoplasmic phosphorylation. J Cell Biol. 2003.

79. Sano Y, Nakaya T, Pedrini S, Takeda S, Iijima-Ando K, Iijima K, et al. Physiological mouse brain Abeta levels are not related to the phosphorylation state of threonine-668 of Alzheimer's APP. PLoS One. 2006.

80. Feyt C, Pierrot N, Tasiaux B, Van Hees J, Kienlen-Campard P, Courtoy PJ, et al. Phosphorylation of APP695 at Thr668 decreases gamma-cleavage and extracellular Abeta. Biochem Biophys Res Commun. 2007.

81. Scheuner D, Eckman C, Jensen M, Song X, Citron M, Suzuki N, et al. Secreted amyloid β–protein similar to that in the senile plaques of Alzheimer's disease is increased in vivo by the presenilin 1 and 2 and APP mutations linked to familial Alzheimer's disease. Nat Med. 1996.

82. Nilsberth C, Westlind-Danielsson A, Eckman CB, Condron MM, Axelman K, Forsell C, et al. The "Arctic" APP mutation (E693G) causes Alzheimer's disease by enhanced Abeta protofibril formation. Nat Neurosci. 2001.

83. Ando K, Iijima KI, Elliott JI, Kirino Y, Suzuki T. Phosphorylation-dependent regulation of the interaction of amyloid precursor protein with Fe65 affects the production of beta-amyloid. J Biol Chem. 2001.

84. Rebelo S, Domingues SC, Santos M, Fardilha M, Esteves SLC, Vieira SI, et al. Identification of a novel complex AβPP:Fe65:PP1 that regulates AβPP Thr668 phosphorylation levels. J Alzheimer's Dis. 2013.

85. Andersson ER, Lendahl U. Therapeutic modulation of Notch signalling--are we there yet? Nat Rev Drug Discov. Nature Publishing Group, a division of Macmillan Publishers Limited. 2014.

7. Appendix

In this section is listed the equipment and solutions used for the experiments developed in this thesis

- Cell Culture

Equipment:

- ✓ Hera cell CO2 incubator (Heraeus)
- ✓ Safety cabinet Hera safe (Heraeus)
- ✓ Inverted optical microscope (LEICA)
- ✓ Sonicator (U200S IKA)
- ✓ Bath SBB6 (Grant)
- ✓ Culture Plates (Corning)

Reagents and Solutions:

- ✓ Complete Medium 10% FBS MEM:F12 (1:1)

MEM (Gibco, Invitrogen)	4.805 g
F12 (Gibco, Invitrogen)	5.315 g
$NaHCO_3$ (Sigma	1.7 g
Sodium Pyruvate (Sigma)	0.055 g
1% Antibiotic/Antimycotic (AA) mix (Gibco, Invitrogen)	10 mL
10% FBS (Gibco, Invitrogen)	100 mL
L-Glutamine (200 mM stock solution)	2.5 mL

Adjust to PH 7.4 and to a final volume of 1000 mL in dH2O. Sterilize by filtering through a 0.2 μm filter and store at 4ºC.

- ✓ PBS (1x)

Dissolve one sack of BupH Modified Dulbecco's Phosphatase Buffered Saline Pack (Pierce) in deionized H2O. Sterilize by filtering through a 0.2 μm filter and store at 4ºC.
Final composition:

Sodium Phosphatase	8 mM

Potassium Phosphatase	2 mM
Sodium Chloride	140 mM
Potassium Chloride	10 mM

- Protein Concentration Determination

Equipment:

- ✓ Infinite M200 (Tecan) and I-ControlTM software
- ✓ 96 well plate (Corning)

Reagents and Solutions:

- ✓ BCA assay kit (Pierce, Rockford, IL)
- ✓ Bovine serum albumin (BSA) (Pierce)
- ✓ Working reagent (50 reagent A: 1 Reagent B)

Reagent A: sodium carbonate, sodium bicarbonate, BCA and sodium tartrate in 0.2 N sodium hydroxide.

Reagent B: 4% cupric sulfate.

- ✓ SDS-PAGE

Equipment:

- ✓ Electrophoresis system (Hoefer SE600 vertical unit)
- ✓ Electrophoresis power supply EPS 1000 (Amersham Pharmacia Biotec)

Reagents and solutions

- ✓ Acrylamide (29:1)

- ✓ UGB (Upper Gel Buffer) (5x)

For 900 mL of deionized H2O add 75.69 g of Tris. Mix until the solute has dissolved. Adjust the PH to 6.8 and the volume to 1 L with deionized H2O.

- LGB (Lower Gel Buffer) (4x)

For 900 mL of deionized H2O add 181.65 g of Tris and 4 g of SDS. Mix until the solute has dissolved. Adjust the PH to 6.8 and the volume to 1 L with deionized H2O.

- 10% APS (Ammonium Persulfate)

In 10 mL of deionized H2O dissolve 1 g of APS.

- 10% SDS (Sodium dodecilsulfate)

In 10 mL of deionized H2O dissolve 1 g of SDS.

- Loading Gel Buffer (LB) (4x)

Tris Solution (PH 6.8) 1mM	2.5 mL (250 mM)
SDS	0.8 g (8%)
Glycerol	4 mL (40%)
Beta-Mercaptoetanol	2 mL (2%)
Bromophenol Blue	1 mg (0.01%)

Adjust the volume to 10 mL with deionized H2O. Store in the dark at room temperature.

- Tris 1M (PH 6.8) solution

For 150 mL of deionized H2O add 30.3 g of Tris base. Adjust the PH to 6.8 and the final volume to 250 mL.

- Running buffer (10x)

Tris	30.3 g (250 mM)
Glycine	144.2 g (2.5 mM)
SDS	10 g (1%)

Dissolve in deionized H2O and adjust the PH to 8.3 and the final volume to 1 L.

- Western-Blotting

Equipment:

- Transphor Electrophoresis unit (Hofer TE 42)
- Electrophoresis power supply EPS 1000 (Amersham Pharmacia Biotec)

Reagents and Solutions:

✓ Transfer buffer (1x)

Tris	3.03 g (25 mM)
Glycine	14.41 g (192 mM)

Mix until the solutes have dissolved. Adjust the PH to 8.3 with HCL and the final volume to 800 mL with deionized H2O. Just before usage add 200 mL of methanol (20%).

✓ Immunoblotting

Reagents and Solutions:

✓ 10x TBS (Tris Buffered Saline)

Tris	12.11 g (10 mM)
NaCl	87.66 g (150 mM)

Adjust the PH to 8.0 with HCL and the final volume to 1 L with deionized H2O.

✓ 10x TBS-T (TBS-Tween 20)

Tris	12.11 g (10 mM)
NaCl	87.66 g (150 mM)
Tween 20	5 mL (0.05%)

Adjust the PH to 8.0 with HCL and the final volume to 1 L with deionized H2O.

✓ Ponceau S solution

Dissolve 0.1 g of Ponceau S (Sigma) in 100 mL of 5% acetic acid solution (5 mL of acetic acid dissolved in 95 mL of deionized H2O).

- ✓ Blocking solution

5% of BSA (Bovine serum albumin, NZytech) in 1x TBS-T.

- ✓ ECL solutions

Luminata crescendo (Millipore)

Home-made ECL

- ✓ Developer and Fixer solutions (Sigma)

- ✓ Membrane stripping solution

Tris-HCL (PH 6.7)	3.76 g (62.5 mM)
SDS	10 g (2%)
Beta-mercaptoethanol	3.5 mL (100 mM)

Dissolve Tris and SDS in deionized H2O and adjust the PH to 6.7. Add the mercaptoethanol and adjust the final volume to 500 mL.

- ✓ Aβ-SDS-PAGE

Equipment:

- ✓ Mini-PROTEAN Tetra Handcast Systems (Biorad)
- ✓ TE70XP Semi-Dry Transfer Unit (Hoefer)
- ✓ Electrophoresis power supply EPS 1000 (Amersham Pharmacia Biotec)

Reagents and solutions

- ✓ Separating Gel Buffer 1.6M Tris/0,4M H2SO4 pH 8,1

Tris-Base	19,38g
0.5M H2SO4	80mL
H2Odd	Until 100mL

- ✓ Stacking Gel Buffer 0.8M Bistris/0,2M H2SO4 pH 6,7

Bistris	8.37g
0.5M H2SO4	20mL
H2Odd	Until 50mL

- ✓ Comb Gel Buffer 0,72M Bistris/0,32M Bicine pH 7.7

Bistris	30.04g
Bicine	10,36g
H2Odd	200mL

- ✓ Rinsing Buffer 0,36M Bistris/0,16M Bicine/0,1% SDS pH 7,7

Comb gel buffer	25mL
1% SDS	5mL
H2Odd	Until 50mL

- ✓ Anode Buffer 200mM Tris/50mM H2SO4 pH8.1

Tris	24.23g
0.5M H2SO4	100mL
H2Odd	Until 1000mL

- ✓ Cathode Buffer 200mM Bicine/100 mM NaOH/0,25% SDS pH8,2

Bicine	32.63g
1M NaOH	100mL
10% SDS	25mL
H2Odd	Until 1000mL

- ✓ Blot Buffer A Stock Solution 2,1M Tris ph 10,4

Tris-Base	127.3g
H2Odd	500mL

- ✓ Blot Buffer B+C Stock Solution 250mM Tris pH 10,4

Tris-Base	30.28g
H2Odd	1000mL

- ✓ 0,5M Boric Acid

Boric Acid	30.9g
H2Odd	1000mL

- ✓ Blot Buffer A 210mM Tis/30%v/v Methanol pH10,4

Blot Buffer A Stock Solution	100mL
Methanol	300mL
H2Odd	Until 1000mL

- ✓ Blot Buffer B 25mM Tris/30%v/v Methanol pH10,4

Blot Buffer B Stock Solution	100mL
Methanol	300mL
H2Odd	Until 1000mL

- ✓ Blot Buffer C 25mM Tris/0.025% SDS pH 9.

Blot Buffer C Stock Solution	200mL
H2O	1600mL
0.5M Boric Acid	20mL
10% SDS	5mL
H2Odd	Until 1000mL